

Inhomogeneous closure and statistical mechanics for Rossby wave turbulence over topography

By JORGEN S. FREDERIKSEN
AND TERENCE J. O'KANE

CSIRO Atmospheric Research, Aspendale, Victoria, Australia

(Received 10 June 2004 and in revised form 30 March 2005)

The quasi-diagonal direct interaction approximation (QDIA) closure theory is formulated for the interaction of mean fields, Rossby waves and inhomogeneous turbulence over topography on a generalized β -plane. An additional small term, corresponding to the solid-body rotation vorticity on the sphere, is included in the barotropic equation and it is shown that this results in a one-to-one correspondence between the dynamical equations, Rossby wave dispersion relations, nonlinear stability criteria and canonical equilibrium theory on the generalized β -plane and on the sphere. The dynamics, kinetic energy spectra, mean field structures and mean streamfunction tendencies contributed by transient eddies are compared with the ensemble-averaged results from direct numerical simulations (DNS) at moderate resolution. A series of numerical experiments is performed to examine the generation of Rossby waves when eastward large-scale flows impinge on a conical mountain in the presence of moderate to strong two-dimensional turbulence. The ensemble predictability of northern hemisphere flows in 10-day forecasts is also examined on a generalized β -plane. In all cases, the QDIA closure is found to be in very good agreement with the statistics of DNS except in situations of strong turbulence and weak mean fields where ensemble-averaged DNS fails to predict mean field amplitudes correctly owing to sampling problems even with as many as 1800 ensemble members.

1. Introduction

The development of modern closures based on renormalized perturbation theory has its origin in the pioneering work of Kraichnan (1958, 1959a) who developed the Eulerian direct interaction approximation (DIA) for homogeneous turbulence. Closely related non-Markovian closures were developed independently by Herring and McComb. Herring's self-consistent field theory (SCFT, Herring 1965) and McComb's local energy transfer theory (LET, McComb 1974; McComb, Filipiak & Shanmugasundaram 1992; McComb & Quinn 2003) have the same equation for the single-time two-point cumulant as the DIA closure, but employ a fluctuation dissipation theorem (FTD, Kraichnan 1959b; Leith 1975; Deker & Haake 1975; Frederiksen & Davies 2000) to relate the two-time cumulants and response functions. These closures and related Markovianized versions such as the eddy-damped quasi-normal Markovian model (EDQNM, Orszag 1970; Leith 1971; Bowman, Krommes & Ottaviani 1993; Frederiksen & Davies 1997), test field model (TFM, Kraichnan 1971a, b; Leith & Kraichnan 1972) and realizable TFM (Bowman & Krommes 1997) have been successfully applied to a variety of important problems. These include comparisons with direct numerical simulations and experimental data (e.g. Herring *et al.* 1974; Pouquet *et al.* 1975; Kraichnan & Herring 1978; McComb 1990; McComb *et al.*

(1992); Frederiksen & Davies 2000, 2004), subgrid-scale parameterizations for eddy viscosity and stochastic backscatter (Kraichnan 1976; Rose 1977; Leith 1990; Chasnov 1991; Frederiksen & Davies 1997; Schilling & Zhou 2002) and the study of the statistics of the predictability of homogeneous turbulent flows (Kraichnan 1970; Leith 1971, 1974; Leith & Kraichnan 1972; Herring 1983; Métais & Lesieur 1986).

Herring (1977) and Holloway (1978, 1987) examined the problem of the interaction of homogeneous turbulence with ensembles of random topography with zero mean value using DIA, TFM and EDQNM closures. These studies elucidated the role that the statistical properties of random topography play in determining spectra of transient vorticity variance and determined a number of spectral subranges with quite different dynamics. However, atmospheric and other geophysical flows often interact with single realization mean topography and tend to be inhomogeneous at the larger scales (Carnevale *et al.* 1995). Kraichnan (1972) formulated generalizations of the DIA and TFM closures to inhomogeneous turbulence interacting with mean fields, but noted that his general non-diagonal form of the inhomogeneous DIA was computationally intractable at any reasonable resolution. Kraichnan (1964*b*) also developed a diagonalizing DIA closure for the special case of Bousinesq convection with a mean horizontally averaged temperature field with zero fluctuations.

Frederiksen (1999) developed a computationally tractable quasi-diagonal DIA (QDIA) closure for flows, with general mean and fluctuating components, over single-realization mean topography on an f -plane and O’Kane & Frederiksen (2004) examined the performance of the closure compared with the statistics of direct numerical simulations (DNS). They found in their experiments that the QDIA for inhomogeneous f -plane two-dimensional turbulence has similar performance to the DIA for homogeneous two-dimensional turbulence (Frederiksen & Davies 2000), that it is only a few times more computationally intensive than the DIA for homogeneous turbulence and that a one-parameter regularized version of the QDIA, in which transfers are localized, is in excellent agreement with DNS at all scales.

Our purpose in this paper is to generalize the QDIA closure theory to the interaction of Rossby wave turbulence with mean fields and topography on a β -plane. In fact, in examining this problem, it became apparent that the standard β -plane approximation neglects a term that corresponds to the solid-body rotation vorticity on the sphere. This term is small compared with the planetary vorticity, but is nevertheless significant for the structure of the dispersion relations of Rossby waves in the presence of mean flows, for the statistical mechanics of Rossby wave turbulence and for closure theory.

The statistical mechanics theory for flow over topography was developed by Salmon, Holloway & Hendershott (1976) in planar geometry and by Frederiksen & Sawford (1981) in spherical geometry. The close relationships between canonical equilibrium solutions and nonlinearly stable steady-state solutions or Fofonoff flows were established in the works of Frederiksen (1982), Frederiksen & Carnevale (1986) and Carnevale & Frederiksen (1987).

One of the primary motivations for developing the QDIA closure (Frederiksen 1999) for inhomogeneous turbulence over topography was to provide a systematic foundation for the development of subgrid-scale parameterizations for the eddy-topographic force based on renormalized perturbation theory. This stress due to the interaction of subgrid-scale eddies with retained scale topography is essential for realistic simulations of ocean circulations (Holloway 1992; Alvarez *et al.* 1994; Merryfield & Holloway 1997, 2002; Kazantsev, Sommeria & Verron 1998; Merryfield, Cummins & Holloway 2001; Polyakov 2001; Chavanis & Sommeria 2002) and also appears to be a missing parameterization in atmospheric circulation models (Frederiksen, Dix & Davies 2003).

Here we re-examine the Rossby wave dispersion relations and statistical mechanics on a generalized β -plane including the contribution from the solid-body rotation vorticity and formulate the QDIA closure on this generalized β -plane. The results for the standard β -plane are recovered by taking the solid-body rotation vorticity to be negligible. We also examine the performance of the QDIA closure in comparison with ensemble-averaged direct numerical simulations (DNS) at moderate resolution for which the wavenumber $k \leq 16$.

In §2, we present the barotropic vorticity equation for flow over topography and Rossby wave turbulence on a generalized β -plane and in the presence of a large-scale flow U . We note the one-to-one correspondence with flow on the sphere both for the dynamical equations and for the Rossby wave dispersion relations. We also discuss the form-drag equation for the large-scale flow U and consider the conserved quantities of kinetic energy and potential enstrophy and the contributions from the large-scale flow and from the ‘small-scales’. In §3, we develop the statistical mechanical equilibrium theory and nonlinear stability theory for flow on the generalized β -plane. In §4, we show how to transform the generalized β -plane equations for the ‘small-scales’ and the large-scale flow U into the standard f -plane form by generalizing the expressions for the interaction coefficients and considering the large-scale flow as a zero wavenumber field. This allows us in §5 to write down the QDIA closure equations on the generalized β -plane in the same form as the f -plane QDIA (Frederiksen 1999) with the sums over wavenumber just extended to include the zero wavenumber component. The QDIA equations in §5 also include contributions from the off-diagonal covariance matrix and from non-Gaussian terms at the initial time. This allows us in the Appendix to formulate a cumulant update version of the QDIA (CUQDIA) which is computationally more efficient (O’Kane & Frederiksen 2004).

In §6, we consider the generation of Rossby waves when large-scale flows interact with isolated topography in the form of a conical mountain located at mid-latitudes. Four different cases of Rossby wave development in the presence of moderate to strong turbulence are considered and the results of large ensembles of DNS are compared with those of the CUQDIA closure. We also consider the role of the contribution to the mean streamfunction tendency from transient eddies in the development of the mean zonally asymmetric streamfunction. In §7, we compare the evolution of ensemble mean fields and the growth of errors within the QDIA closure and DNS during ensemble forecasts on a generalized β -plane. The implications of our results and our conclusions are summarized in §8.

2. Two-dimensional flow on a generalized β -plane

The differential rotation rate plays an important role in the interaction of mean flows, turbulence and topography in many geophysical fluid dynamics contexts. Here we include this effect through the β -plane approximation generalized to include a term representing the solid-body rotation vorticity of the corresponding spherical geometry problem. As in the analogous standard β -plane problem (Carnevale & Frederiksen 1987; Frederiksen & Frederiksen 1989) we represent the full streamfunction $\Psi = \psi - Uy$, where U is a large-scale east–west flow and ψ represents the ‘small scales’. The evolution equation for two-dimensional motion of the ‘small scales’ over a mean topography on a generalized β -plane is described by the barotropic vorticity equation

$$\frac{\partial \zeta}{\partial t} = -J(\psi - Uy, \zeta + h + \beta y + k_0^2 Uy) + \hat{v} \nabla^2 \zeta + f^0. \quad (2.1a)$$

Here, f^0 is the bare forcing, $\hat{\nu}$ the bare viscosity,

$$J(\psi, \zeta) = \frac{\partial \psi}{\partial x} \frac{\partial \zeta}{\partial y} - \frac{\partial \psi}{\partial y} \frac{\partial \zeta}{\partial x} \quad (2.1b)$$

is the Jacobian and k_0 is a wavenumber that specifies the strength of the large-scale vorticity corresponding to the solid-body rotation on a sphere. The vorticity is the Laplacian of the streamfunction $\zeta = \nabla^2 \psi$. We assume that the variation in the topography (ΔH) is small, and define h to be the scaled spatial variation of the height of the topography relative to the total depth. The barotropic vorticity equation can be made non-dimensional by introducing suitable length and time scales as specified in §6.

The standard β -plane vorticity equation is obtained by setting k_0^2 to zero. We note, however, that there is a one-to-one correspondence between the generalized β -plane equation and that for flow on the sphere in the presence of a solid-body rotation contribution. The structural equivalence is most easily seen by choosing a length scale of a , the earth's radius, and a time scale of Ω^{-1} , the inverse of the earth's angular velocity, for deriving the non-dimensional spherical barotropic vorticity equation. Then these equations are equivalent, with ζ replaced by the total vorticity on the sphere and with the replacements $x \rightarrow \lambda$, the longitude, $y \rightarrow \sin \phi$, the sine of the latitude, $\beta y \rightarrow 2 \sin \phi$ and $k_0^2 U y \rightarrow 2U \sin \phi$ (Frederiksen & Frederiksen 1991). This last term, corresponding to the solid-body rotation vorticity, arises from the fact that $\nabla_{sphere}^2(-U \sin \phi) = 2U \sin \phi$ and makes a small but structurally important addition to the planetary vorticity $2 \sin \phi$.

In this paper, we consider the barotropic vorticity equation on the doubly periodic domain ($0 \leq x \leq 2\pi$), ($0 \leq y \leq 2\pi$). We derive the corresponding spectral space equations by representing each of 'small-scale' terms by a Fourier series; for example

$$\zeta(\mathbf{x}, t) = \sum_{\mathbf{k}} \zeta_{\mathbf{k}}(t) \exp(i\mathbf{k} \cdot \mathbf{x}), \quad (2.2a)$$

where

$$\zeta_{\mathbf{k}}(t) = \frac{1}{(2\pi)^2} \int_0^{2\pi} \int_0^{2\pi} d^2 \mathbf{x} \zeta(\mathbf{x}, t) \exp(-i\mathbf{k} \cdot \mathbf{x}) \quad (2.2b)$$

and $\mathbf{x} = (x, y)$, $\mathbf{k} = (k_x, k_y)$, $k = (k_x^2 + k_y^2)^{1/2}$ and $\zeta_{-\mathbf{k}}$ is conjugate to $\zeta_{\mathbf{k}}$.

2.1. Dispersion relations for Rossby waves

Individual Rossby waves of the form $\exp(i(\mathbf{k} \cdot \mathbf{x} - \omega_{\mathbf{k}}^U t))$ are solutions of the corresponding inviscid unforced homogeneous equation, obtained by setting $h=0$, $\hat{\nu}=0$ and $f^0=0$ in (2.1), provided the Doppler shifted frequency satisfies the dispersion relation

$$\omega_{\mathbf{k}}^U = k_x U - \frac{\beta k_x + k_0^2 U k_x}{k^2}. \quad (2.3)$$

We note that the Rossby wave frequency on the generalized β -plane has the same form as on the sphere with the replacements $k_x \rightarrow m$, $\beta \rightarrow 2$, $k_0^2 \rightarrow 2$ and $k^2 \rightarrow n(n+1)$ where m and n are the zonal and the total wavenumbers of Rossby waves on the sphere (Frederiksen 1982). In contrast, on the standard β -plane, k_0^2 vanishes.

2.2. Large-scale flow equation and conservation laws

The form-drag equation for the large-scale flow U is the same as on the standard β -plane (Carnevale & Frederiksen 1987). With the inclusion of relaxation towards

the state \bar{U} , it takes the form

$$\frac{\partial U}{\partial t} = \frac{1}{S} \int_S h \frac{\partial \psi}{\partial x} dS + \alpha(\bar{U} - U). \quad (2.4)$$

Here, α is a drag coefficient and S is the area of the surface $0 \leq x \leq 2\pi$, $0 \leq y \leq 2\pi$. In the absence of forcing and dissipation (2.1) and (2.4) together conserve kinetic energy and potential enstrophy. The kinetic energy is given by

$$E = \frac{1}{2} U^2 + \frac{1}{2} \frac{1}{S} \int_S (\nabla \psi)^2 dS, \quad (2.5)$$

while the potential enstrophy is defined by

$$\begin{aligned} Q &= \frac{1}{2} \left(k_0 U + \frac{\beta}{k_0} \right)^2 + \frac{1}{2} \frac{1}{S} \int_S (\zeta + h)^2 dS, \\ &= \frac{1}{2} (\zeta_U + h_U)^2 + \frac{1}{2} \frac{1}{S} \int_S (\zeta + h)^2 dS, \end{aligned} \quad (2.6)$$

where $\zeta_U = k_0 U$ and $h_U = \beta/k_0$. Again, the expressions (2.5) and (2.6) for the kinetic energy and potential enstrophy have the same forms as on the sphere (Frederiksen & Carnevale 1986). The ‘small scale’ contributions are also the same as in (5.9) of Carnevale & Frederiksen (1987), but on the standard β -plane, the potential enstrophy contribution from the large-scale flow is the unusual term βU . Note that on the generalized β -plane, the large-scale flow contributes the additional non-trivial term $k_0^2 U^2/2$ and the trivial constant term $\beta^2/2k_0^2$.

3. Canonical equilibrium theory and nonlinear stability

Next, we examine the equilibrium statistical mechanics of flow over topography on the generalized β -plane and compare our results with those of Carnevale & Frederiksen (1987) for flow on the standard β -plane. It is also shown that in the limit as $k_0 \rightarrow 0$, the canonical equilibrium solutions on the generalized β -plane reduce to those on the standard β -plane. The result of Carnevale & Frederiksen (1987), that in the limit of infinite resolution the canonical mean state is statistically sharp and identical to the nonlinearly stable minimum enstrophy state, applies equally well on the generalized β -plane.

3.1. Generalized β -plane

First, we consider stationary solutions to (2.1a) (with $\hat{v} = 0$ and $f^0 = 0$) for which the potential enstrophy is proportional to the streamfunction. Thus, as in (5.10) of Carnevale & Frederiksen (1987)

$$\mu(\psi^S - U^S y) = \nabla^2 \psi^S + \beta y + k_0^2 U^S y + h, \quad (3.1)$$

where μ is the constant of proportionality. From (3.1), we see that the large-scale contributions may be separated and written as

$$\mu = \frac{\beta + k_0^2 U^S}{U^S} \quad (3.2)$$

or

$$U^S = -\frac{\beta}{\mu + k_0^2} = -\frac{k_0 h_U}{\mu + k_0^2}. \quad (3.3)$$

According to the nonlinear stability theory of Arnold (1965), stationary states determined by the criterion (3.1) are nonlinearly stable provided $\mu > -k_0^2$, where k_0 is the smallest retained wavenumber or if $\mu < -k_{max}^2$ where k_{max} is the largest retained wavenumber. The first branch of solutions have minimum potential enstrophy Q for a given energy E , while on the second branch, the potential enstrophy is a maximum. However, the maximum potential enstrophy branch is not relevant in the physically interesting limit $k_{max} \rightarrow \infty$.

Now the kinetic energy and potential enstrophy of the large-scale flow are given by

$$E_U = \frac{1}{2}U^2 \quad (3.4)$$

and

$$Q_U = \frac{1}{2} \left(k_0 U + \frac{\beta}{k_0} \right)^2 = \frac{1}{2} (\zeta_U + h_U)^2. \quad (3.5)$$

Thus the contributions from the large-scale flow to the stationary kinetic energy and enstrophy can be written as

$$E_U^S = \frac{1}{2} \frac{\beta^2}{(\mu + k_0^2)^2} = \frac{\frac{1}{2} k_0^2 |h_U|^2}{(\mu + k_0^2)^2}, \quad (3.6)$$

$$Q_U^S = \frac{1}{2} (k_0 U^S + h_U)^2 = \frac{\frac{1}{2} \mu^2 |h_U|^2}{(\mu + k_0^2)^2}. \quad (3.7)$$

Consequently, the total stationary kinetic energy and enstrophy take the form

$$E^S = \frac{\frac{1}{2} k_0^2 |h_U|^2}{(\mu + k_0^2)^2} + \frac{1}{2} \sum_k \frac{k^2 |h_k|^2}{(\mu + k^2)^2}, \quad (3.8)$$

$$Q^S = \frac{\frac{1}{2} \mu^2 |h_U|^2}{(\mu + k_0^2)^2} + \frac{1}{2} \sum_k \frac{\mu^2 |h_k|^2}{(\mu + k^2)^2}. \quad (3.9)$$

We see that the large-scale flow just adds extra terms of the same form as the expression for the small scales, but with the replacements $k^2 \rightarrow k_0^2$ and $h_k \rightarrow h_U$. As noted by Frederiksen & Carnevale (1986) and Carnevale & Frederiksen (1987), the solution to (3.1) also gives the stationary contribution to the canonical equilibrium spectrum if $\mu \rightarrow \mu^{eq} = a/b$ where a and b are parameters determined by the conserved values of kinetic energy E and potential enstrophy Q . With this replacement, the stationary contributions to the canonical equilibrium energy and potential enstrophy are again given by (3.8) and (3.9). In general, μ^{eq} is different from μ , but as shown by Carnevale & Frederiksen (1987), in the limit of infinite resolution, these two parameters are identical and this result applies equally on the generalized β -plane.

The expressions for the kinetic energy and potential enstrophy in (2.5), (2.6), (3.4) and (3.5) are in the standard form for the application of statistical mechanical equilibrium theory, as outlined in §2 of Frederiksen & Sawford (1981). We find that the large-scale flow contributions to the transient terms are

$$E_U^T = \frac{\frac{1}{2}}{a + b k_0^2}, \quad (3.10)$$

$$Q_U^T = \frac{\frac{1}{2} k_0^2}{a + b k_0^2}, \quad (3.11)$$

and the total transient kinetic energy and potential enstrophy are given by

$$E^T = \frac{\frac{1}{2}}{a + bk_0^2} + \frac{1}{2} \sum_k \frac{1}{a + bk^2}, \quad (3.12)$$

$$Q^T = \frac{\frac{1}{2}k_0^2}{a + bk_0^2} + \frac{1}{2} \sum_k \frac{k^2}{a + bk^2}. \quad (3.13)$$

Again, the large-scale flow simply adds an extra term with $k^2 \rightarrow k_0^2$. Also note that with $\zeta_U = k_0 U$, it is found that

$$\langle \zeta_U \rangle = k_0 U^s = \frac{-bk_0^2 h_U}{a + bk_0^2}, \quad (3.14)$$

which is in the same form as (13.1a) of Frederiksen (1999) with $k^2 \rightarrow k_0^2$, $h_k \rightarrow h_U$.

The parameters a and b are obtained from (3.8), (3.9), (3.12) and (3.13) by equating the total kinetic energy $E = E^s + E^T$ and the total potential enstrophy $Q = Q^s + Q^T$ to their initial specified values. From (3.8) and (3.9), it is evident that positivity of energy and potential enstrophy means that $a + bk^2 > 0$ for all k . Again the conditions for the existence of the canonical equilibrium solutions are $\mu^{eq} > -k_0^2$ or $\mu^{eq} < -k_{max}^2$ and thus correspond to the same ranges as for nonlinear stability.

Throughout this paper, we shall be concerned with finite-resolution spectrally truncated flows for which the canonical equilibrium and nonlinear stability theories are as described above. We note, however, that for the corresponding continuum dynamics of fluids, more general nonlinear stable structures are possible because of the infinity of dynamical invariants that then exist. Carnevale & Frederiksen (1987) have shown that it is then also possible to generalize the two-invariant energy-potential enstrophy statistical mechanics to construct more general canonical distributions which are consistent with the general many-invariant nonlinearly stable structures. Generalized many-invariant statistical mechanical equilibrium states have been applied to Jupiter's red spot (Miller, Weichman & Cross 1992; Turkington *et al.* 2001), to magneto-hydrodynamics (Isichenko & Gruzinov 1994) and to two-dimensional flows and turbulence (e.g. Majda & Holen 1997; Ellis, Haven & Turkington 2002; Abramov & Majda 2003).

3.2. Standard β -plane

The potential enstrophy for the standard β -plane ((5.12b) of Carnevale & Frederiksen 1987) differs from that on the generalized β -plane by a constant term $(\beta/k_0)^2/2$ as well as by the term $k_0^2 U^2/2$. We subtract the trivial constant term from the potential enstrophy of the large-scale flow to define

$$\tilde{Q}_U = Q_U - \frac{1}{2}(\beta/k_0)^2, \quad (3.15)$$

$$\begin{aligned} \tilde{Q}_U^s &= \frac{\frac{1}{2}\mu^2(\beta/k_0)^2}{(\mu + k_0^2)^2} - \frac{1}{2}(\beta/k_0)^2 \\ &= -\frac{\beta^2\mu + \frac{1}{2}\beta^2k_0^2}{(\mu + k_0^2)^2}. \end{aligned} \quad (3.16)$$

We then find that

$$\tilde{Q}_U^s \rightarrow -\frac{\beta^2}{\mu}, \quad Q_U^T \rightarrow 0, \quad (3.17)$$

as $k_0^2 \rightarrow 0$ and we recover the results of Carnevale & Frederiksen (1987) for the standard β -plane.

4. Transformation of β -plane spectral equations into f -plane form

Next, we present the spectral equations for the ‘small scales’ on the generalized β -plane and show that these equations and (2.4) for the large-scale flow can be combined and written in the form of the f -plane spectral equations (Frederiksen 1999; O’Kane & Frederiksen 2004). This is established by defining suitable interaction coefficients, representing the large-scale flow as a component with zero wavenumber and extending the sums over wavenumbers. This allows us in § 5 and in the Appendix to develop the generalized β -plane QDIA closure equations from the f -plane theory. We use (2.2) to represent the barotropic vorticity equation (2.1) in spectral form

$$\begin{aligned} \left(\frac{\partial}{\partial t} + \nu_0(\mathbf{k})k^2 \right) \zeta_{\mathbf{k}}(t) &= \sum_{\mathbf{p} \in \mathbf{R}} \sum_{\mathbf{q} \in \mathbf{R}} \delta(\mathbf{k} + \mathbf{p} + \mathbf{q}) [K(\mathbf{k}, \mathbf{p}, \mathbf{q}) \zeta_{-\mathbf{p}} \zeta_{-\mathbf{q}} + A(\mathbf{k}, \mathbf{p}, \mathbf{q}) \zeta_{-\mathbf{p}} h_{-\mathbf{q}}] \\ &\quad + f_{\mathbf{k}}^0 - [ik_x U(\zeta_{\mathbf{k}} + h_{\mathbf{k}}) + ik_x \psi_{\mathbf{k}} k_0^2 U] \\ &= \sum_{\mathbf{p} \in \mathbf{R}} \sum_{\mathbf{q} \in \mathbf{R}} \delta(\mathbf{k} + \mathbf{p} + \mathbf{q}) [K(\mathbf{k}, \mathbf{p}, \mathbf{q}) \zeta_{-\mathbf{p}} \zeta_{-\mathbf{q}} + A(\mathbf{k}, \mathbf{p}, \mathbf{q}) \zeta_{-\mathbf{p}} h_{-\mathbf{q}}] \\ &\quad + f_{\mathbf{k}}^0 + k_0 \left[\frac{k_x}{k^2} - \frac{k_x}{k_0^2} \right] \zeta_{\mathbf{k}} \zeta_{-\mathbf{0}} + k_0 \left[\frac{k_x}{k^2} \zeta_{\mathbf{k}} h_{-\mathbf{0}} - \frac{k_x}{k_0^2} \zeta_{-\mathbf{0}} h_{\mathbf{k}} \right]. \end{aligned} \quad (4.1)$$

Here, $f_{\mathbf{k}}^0$ is the bare forcing, and the complex $\nu_0(\mathbf{k})$ is related to the bare viscosity $\hat{\nu}$ and the intrinsic Rossby wave frequency $\omega_{\mathbf{k}}$ by the expression:

$$\nu_0(\mathbf{k})k^2 = \hat{\nu}k^2 + i\omega_{\mathbf{k}}, \quad (4.2)$$

where

$$\omega_{\mathbf{k}} = -\frac{\beta k_x}{k^2}. \quad (4.3)$$

Also, we have defined

$$\zeta_{-\mathbf{0}} = ik_0 U, \quad \zeta_{\mathbf{0}} = \zeta_{-\mathbf{0}}^*, \quad (4.4)$$

and introduced a term $h_{-\mathbf{0}}$ that we take to be zero, but which could more generally be related to a large-scale topography. We note that U is real and we have defined $\zeta_{\mathbf{0}}$ to be imaginary. This ensures that all the interaction coefficients that we use are defined to be purely real. It is then possible to extend the sums over \mathbf{p} and \mathbf{q} to include the vector $\mathbf{0}$, to define appropriate real interaction coefficients and map the β -plane problem into the same form as the f -plane problem. Note that we distinguish between $\mathbf{0}$ and $-\mathbf{0}$ in this representation and these components are complex conjugates as is the case for the ‘small-scale’ components with oppositely signed wave vectors (equation (2.2)). The set \mathbf{R} consists of all points in discrete wavenumber space except the point (0,0).

The interaction coefficients required in (4.1) are defined by

$$A(\mathbf{k}, \mathbf{p}, \mathbf{q}) = -\gamma(p_x \hat{q}_y - \hat{p}_y q_x) / p^2, \quad (4.5)$$

$$K(\mathbf{k}, \mathbf{p}, \mathbf{q}) = \frac{1}{2}[A(\mathbf{k}, \mathbf{p}, \mathbf{q}) + A(\mathbf{k}, \mathbf{q}, \mathbf{p})] = \frac{1}{2}\gamma[p_x \hat{q}_y - \hat{p}_y q_x](p^2 - q^2) / p^2 q^2 \quad (4.6)$$

and

$$\delta(\mathbf{k} + \mathbf{p} + \mathbf{q}) = \begin{cases} 1 & \text{if } \mathbf{k} + \mathbf{p} + \mathbf{q} = \mathbf{0}, \\ 0 & \text{otherwise.} \end{cases} \quad (4.7)$$

In fact, our definitions of the interaction coefficients are generalized to include the zero wave vector as any of the three arguments by specifying γ , \hat{q}_y and \hat{p}_y as follows:

$$\gamma = \begin{cases} -\frac{1}{2}k_0 & \text{if } \mathbf{k} = \mathbf{0}, \\ k_0 & \text{if } \mathbf{q} = \mathbf{0} \text{ or } \mathbf{p} = \mathbf{0}, \\ 1 & \text{otherwise,} \end{cases} \quad (4.8)$$

$$\hat{q}_y = \begin{cases} 1 & \text{if } \mathbf{k} = \mathbf{0} \text{ or } \mathbf{p} = \mathbf{0} \text{ or } \mathbf{q} = \mathbf{0}, \\ q_y & \text{otherwise,} \end{cases} \quad (4.9)$$

$$\hat{p}_y = \begin{cases} 1 & \text{if } \mathbf{k} = \mathbf{0} \text{ or } \mathbf{p} = \mathbf{0} \text{ or } \mathbf{q} = \mathbf{0}, \\ p_y & \text{otherwise.} \end{cases} \quad (4.10)$$

We note that the interaction coefficients satisfy the following relationships:

$$A(-\mathbf{k}, -\mathbf{p}, -\mathbf{q}) = A(\mathbf{k}, \mathbf{p}, \mathbf{q}), \quad (4.11)$$

$$K(-\mathbf{k}, -\mathbf{p}, -\mathbf{q}) = K(\mathbf{k}, \mathbf{p}, \mathbf{q}), \quad (4.12)$$

and

$$K(\mathbf{k}, \mathbf{p}, \mathbf{q}) + K(\mathbf{p}, \mathbf{q}, \mathbf{k}) + K(\mathbf{q}, \mathbf{k}, \mathbf{p}) = 0, \quad (4.13)$$

for all \mathbf{k} , \mathbf{p} and \mathbf{q} including the zero vectors.

The spectral form of the barotropic vorticity equation with differential rotation, describing the evolution of the ‘small scales’, may then be written in the same compact form as for the f -plane:

$$\left(\frac{\partial}{\partial t} + \nu_0(\mathbf{k})k^2 \right) \zeta_{\mathbf{k}}(t) = \sum_{\mathbf{p} \in \mathbf{T}} \sum_{\mathbf{q} \in \mathbf{T}} \delta(\mathbf{k} + \mathbf{p} + \mathbf{q}) [K(\mathbf{k}, \mathbf{p}, \mathbf{q}) \zeta_{-\mathbf{p}} \zeta_{-\mathbf{q}} + A(\mathbf{k}, \mathbf{p}, \mathbf{q}) \zeta_{-\mathbf{p}} h_{-\mathbf{q}}] + f_{\mathbf{k}}^0, \quad (4.14)$$

where $\mathbf{T} = \mathbf{R} \cup \mathbf{0}$.

It remains to show that the form-drag equation for the large-scale flow can also be written in this form. From (2.4) we have

$$\frac{\partial U}{\partial t} = -i \sum_{\mathbf{q} \in \mathbf{R}} \frac{q_x}{q^2} \zeta_{\mathbf{q}} h_{-\mathbf{q}} + \alpha(\bar{U} - U), \quad (4.15)$$

$$\frac{\partial U}{\partial t} = -i \frac{1}{2} \sum_{\mathbf{p} \in \mathbf{R}} \sum_{\mathbf{q} \in \mathbf{R}} \delta(\mathbf{0} + \mathbf{p} + \mathbf{q}) \frac{(p_x - q_x)}{p^2} \zeta_{-\mathbf{p}} h_{-\mathbf{q}} + \alpha(\bar{U} - U). \quad (4.16)$$

Thus,

$$\frac{\partial \zeta_{\mathbf{0}}}{\partial t} = -k_0 \frac{1}{2} \sum_{\mathbf{p} \in \mathbf{R}} \sum_{\mathbf{q} \in \mathbf{R}} \delta(\mathbf{0} + \mathbf{p} + \mathbf{q}) \frac{(p_x - q_x)}{p^2} \zeta_{-\mathbf{p}} h_{-\mathbf{q}} + \alpha(\bar{\zeta}_{\mathbf{0}} - \zeta_{\mathbf{0}}(t)), \quad (4.17)$$

since $\zeta_{\mathbf{0}} = -ik_0 U$ and $\bar{\zeta}_{\mathbf{0}} = -ik_0 \bar{U}$. This means that

$$\left(\frac{\partial}{\partial t} + \nu_0(\mathbf{k}_0)k_0^2 \right) \zeta_{\mathbf{0}}(t) = \sum_{\mathbf{p} \in \mathbf{T}} \sum_{\mathbf{q} \in \mathbf{T}} \delta(\mathbf{0} + \mathbf{p} + \mathbf{q}) [K(\mathbf{0}, \mathbf{p}, \mathbf{q}) \zeta_{-\mathbf{p}} \zeta_{-\mathbf{q}} + A(\mathbf{0}, \mathbf{p}, \mathbf{q}) \zeta_{-\mathbf{p}} h_{-\mathbf{q}}] + f_{\mathbf{0}}^0, \quad (4.18)$$

on using the definitions and properties of the interaction coefficients in (4.5) to (4.13). In particular, we note that

$$\sum_{\mathbf{p} \in \mathbf{R}} \sum_{\mathbf{q} \in \mathbf{R}} \delta(\mathbf{0} + \mathbf{p} + \mathbf{q}) K(\mathbf{0}, \mathbf{p}, \mathbf{q}) \zeta_{-\mathbf{p}} \zeta_{-\mathbf{q}} = 0. \quad (4.19)$$

Here, f_0^0 and $v_0(\mathbf{k}_0)$ are defined by

$$f_0^0 = \alpha \bar{\zeta}_0, \quad (4.20)$$

$$v_0(\mathbf{k}_0) k_0^2 = \alpha. \quad (4.21)$$

Finally, we see that (4.18) for the large-scale flow is in the same form as (4.14) for the 'small scales' and as in (2.3) of Frederiksen (1999) for the f -plane. Thus (4.14) holds for all \mathbf{k} in the set $\mathbf{T} = \mathbf{R} \cup \mathbf{0}$.

5. QDIA closure equations

The method of deriving the QDIA closure equations from (4.14), with \mathbf{k} in the set $\mathbf{T} = \mathbf{R} \cup \mathbf{0}$, is exactly as described by Frederiksen (1999). Here, we briefly motivate the derivation and further elaborate on the closure equations in the Appendix. Suppose we have an ensemble of flows satisfying (4.14) and we express the vorticity $\zeta_{\mathbf{k}}$ and forcing $f_{\mathbf{k}}^0$ in terms of their ensemble means, denoted by $\langle \rangle$, and the deviations from the ensemble mean, denoted by $\hat{\ }:$

$$\zeta_{\mathbf{k}} = \langle \zeta_{\mathbf{k}} \rangle + \hat{\zeta}_{\mathbf{k}}, \quad (5.1a)$$

$$f_{\mathbf{k}}^0 = \langle f_{\mathbf{k}}^0 \rangle + \hat{f}_{\mathbf{k}}^0. \quad (5.1b)$$

The equations for the ensemble mean and the deviation can then be written in the form:

$$\begin{aligned} \left(\frac{\partial}{\partial t} + v_0(\mathbf{k}) k^2 \right) \langle \zeta_{\mathbf{k}} \rangle &= \sum_{\mathbf{p}} \sum_{\mathbf{q}} \delta(\mathbf{k} + \mathbf{p} + \mathbf{q}) K(\mathbf{k}, \mathbf{p}, \mathbf{q}) [\langle \zeta_{-\mathbf{p}} \rangle \langle \zeta_{-\mathbf{q}} \rangle + C_{-\mathbf{p}, -\mathbf{q}}(t, t)] \\ &\quad + \sum_{\mathbf{p}} \sum_{\mathbf{q}} \delta(\mathbf{k} + \mathbf{p} + \mathbf{q}) A(\mathbf{k}, \mathbf{p}, \mathbf{q}) \langle \zeta_{-\mathbf{p}} \rangle h_{-\mathbf{q}} + \langle f_{\mathbf{k}}^0 \rangle, \end{aligned} \quad (5.2a)$$

$$\begin{aligned} \left(\frac{\partial}{\partial t} + v_0(\mathbf{k}) k^2 \right) \hat{\zeta}_{\mathbf{k}} &= \sum_{\mathbf{p}} \sum_{\mathbf{q}} \delta(\mathbf{k} + \mathbf{p} + \mathbf{q}) K(\mathbf{k}, \mathbf{p}, \mathbf{q}) \\ &\quad \times [\langle \zeta_{-\mathbf{p}} \rangle \hat{\zeta}_{-\mathbf{q}} + \hat{\zeta}_{-\mathbf{p}} \langle \zeta_{-\mathbf{q}} \rangle + \hat{\zeta}_{-\mathbf{p}} \hat{\zeta}_{-\mathbf{q}} - C_{-\mathbf{p}, -\mathbf{q}}(t, t)] \\ &\quad + \sum_{\mathbf{p}} \sum_{\mathbf{q}} \delta(\mathbf{k} + \mathbf{p} + \mathbf{q}) A(\mathbf{k}, \mathbf{p}, \mathbf{q}) \hat{\zeta}_{-\mathbf{p}} h_{-\mathbf{q}} + \hat{f}_{\mathbf{k}}^0. \end{aligned} \quad (5.2b)$$

Here, the two-point cumulant is defined by

$$C_{-\mathbf{p}, -\mathbf{q}}(t, s) = \langle \hat{\zeta}_{-\mathbf{p}}(t) \hat{\zeta}_{-\mathbf{q}}(s) \rangle \quad (5.3)$$

and throughout this section and the Appendix, \mathbf{p} and \mathbf{q} both range over the set $\mathbf{T} = \mathbf{R} \cup \mathbf{0}$.

Thus, we see from (5.2a) that to determine the mean field, we require an equation for the two-point cumulant $C_{-\mathbf{p}, -\mathbf{q}}(t, t)$. However, the cost of computing the full covariance matrix is prohibitive at any reasonable resolution (Kraichnan 1972). The quasi-diagonal DIA closure equations (QDIA, Frederiksen 1999) instead express the off-diagonal two-point cumulant and response functions in terms of the diagonal

elements. The resulting equations for the mean field, two-point cumulant and response functions are expressed entirely in terms of the diagonal elements of the two-point cumulant and response functions and are computationally much more efficient than the general inhomogeneous closure equations (Kraichnan 1972).

In the QDIA approach, \hat{f}_k^0 and $\nu_0(\mathbf{k})k^2$ are regarded as order unity ((A.2) of Frederiksen 1999) and the nonlinear and bilinear terms in (5.2b) are treated perturbatively prior to renormalization. This results in the following first-order expression for the off-diagonal elements of the covariance matrix (Frederiksen 1999):

$$\begin{aligned} C_{k,-l}(t, t') &= \int_{t_0}^t ds R_k(t, s) C_l(s, t') [A(\mathbf{k}, -\mathbf{l}, \mathbf{l} - \mathbf{k}) h_{(k-l)} + 2K(\mathbf{k}, -\mathbf{l}, \mathbf{l} - \mathbf{k}) \langle \zeta_{(k-l)}(s) \rangle] \\ &+ \int_{t_0}^{t'} ds R_{-l}(t', s) C_k(t, s) [A(-\mathbf{l}, \mathbf{k}, \mathbf{l} - \mathbf{k}) h_{(k-l)} + 2K(-\mathbf{l}, \mathbf{k}, \mathbf{l} - \mathbf{k}) \langle \zeta_{(k-l)}(s) \rangle] \\ &+ R_k(t, t_0) R_{-l}(t', t_0) \tilde{K}_{k,-l}^{(2)}(t_0, t_0), \end{aligned} \quad (5.4)$$

where $\tilde{K}_{k,-l}^{(2)}(t_0, t_0)$ is the contribution to the off-diagonal covariance matrix at initial time t_0 (O'Kane 2003; O'Kane & Frederiksen 2004). Similarly, the off-diagonal elements of the response function take the form

$$R_{k,l}(t, t') = \int_{t'}^t ds R_k(t, s) R_l(s, t') [A(\mathbf{k}, -\mathbf{l}, \mathbf{l} - \mathbf{k}) h_{(k-l)} + 2K(\mathbf{k}, -\mathbf{l}, \mathbf{l} - \mathbf{k}) \langle \zeta_{(k-l)}(s) \rangle], \quad (5.5)$$

as in (A.12) of Frederiksen (1999). Here, the response function measures the change in the vorticity perturbation owing to an infinitesimal change in the forcing:

$$R_{k,l}(t, t') = \left\langle \frac{\delta \hat{\zeta}_k(t)}{\delta \hat{f}_l^0(t')} \right\rangle. \quad (5.6a)$$

We also use the abbreviations

$$C_k(t, t') = C_{k,-k}(t, t'), \quad R_k(t, t') = R_{k,k}(t, t'). \quad (5.6b)$$

Then, using (5.4) in (5.2a), we obtain the mean field equation, to second order in renormalized perturbation theory. It can also be written in the form given in (A 1) of the Appendix.

Multiplying (5.2b) by $\hat{\zeta}_{-k}(t')$ and averaging leads to the second-order expression for the diagonal two-time cumulant in terms of two- and three-point terms

$$\begin{aligned} \left(\frac{\partial}{\partial t} + \nu_0(\mathbf{k})k^2 \right) C_k(t, t') &= \sum_p \sum_q \delta(\mathbf{k} + \mathbf{p} + \mathbf{q}) A(\mathbf{k}, \mathbf{p}, \mathbf{q}) C_{-p-k}(t, t') h_{-q} \\ &+ \sum_p \sum_q \delta(\mathbf{k} + \mathbf{p} + \mathbf{q}) K(\mathbf{k}, \mathbf{p}, \mathbf{q}) \times [\langle \zeta_{-p}(t) \rangle C_{-q-k}(t, t') \\ &+ C_{-p-k}(t, t') \langle \zeta_{-q}(t) \rangle + \langle \hat{\zeta}_{-p}(t) \hat{\zeta}_{-q}(t) \hat{\zeta}_{-k}(t') \rangle] \\ &+ \int_{t_0}^{t'} ds F_k^0(t, s) R_{-k}(t', s), \end{aligned} \quad (5.7)$$

where $F_k^0(t, s) = \langle \hat{f}_k^0(t) \hat{f}_k^{0*}(s) \rangle$ is the random forcing. To close this equation, we also need an expression for the three-point cumulant and this is derived in the same way as for the DIA closure for homogeneous turbulence (Kraichnan 1959a; Frederiksen &

Davies 2000):

$$\begin{aligned}
\langle \hat{\zeta}_{-l}(t) \hat{\zeta}_{(l-k)}(t) \hat{\zeta}_k(t') \rangle &= 2 \int_{t_0}^{t'} ds K(\mathbf{k}, -l, l-k) C_{-l}(t, s) C_{(l-k)}(t, s) R_k(t', s) \\
&+ 2 \int_{t_0}^t ds K(-l, l-k, \mathbf{k}) R_{-l}(t, s) C_{(l-k)}(t, s) C_k(t', s) \\
&+ 2 \int_{t_0}^t ds K(l-k, -l, \mathbf{k}) R_{(l-k)}(t, s) C_{-l}(t, s) C_k(t', s) \\
&+ R_{-l}(t, t_0) R_{(l-k)}(t, t_0) R_k(t, t_0) \tilde{K}_{-l, (l-k), k}^{(3)}(t_0, t_0, t_0), \quad (5.8)
\end{aligned}$$

where $\tilde{K}_{-l, (l-k), k}^{(3)}(t_0, t_0, t_0)$ allows for non-Gaussian initial conditions. The prognostic equation for $C_k(t, t')$ can also be written as described in the Appendix.

Finally, we need an equation for the diagonal response function $R_k(t, t')$ and this is given by

$$\begin{aligned}
\left(\frac{\partial}{\partial t} + \nu_0(\mathbf{k})k^2 \right) R_k(t, t') &= \int_{t'}^t ds \sum_p \sum_q \delta(\mathbf{k} + \mathbf{p} + \mathbf{q}) R_k(s, t') R_{-p}(t, s) \\
&\times \{ 4K(\mathbf{k}, \mathbf{p}, \mathbf{q}) K(-\mathbf{p}, -\mathbf{k}, -\mathbf{q}) C_{-q}(t, s) \\
&+ [2K(\mathbf{k}, \mathbf{p}, \mathbf{q}) \langle \zeta_{-q}(t) \rangle + A(\mathbf{k}, \mathbf{p}, \mathbf{q}) h_{-q}] \\
&\times [2K(-\mathbf{p}, -\mathbf{k}, -\mathbf{q}) \langle \zeta_q(s) \rangle + A(-\mathbf{p}, -\mathbf{k}, -\mathbf{q}) h_q] \} \quad (5.9)
\end{aligned}$$

(Frederiksen 1999) with $R_k(t, t) = 1$ and $R_k(t, t') = 0$ for $t < t'$.

We could also obtain an expression for $C_{k, -l}(t, t')$ to second order in renormalized perturbation theory by multiplying (5.2b) by $\hat{\zeta}_{-l}(t')$ and averaging; but its computation would be expensive and is not required for our purposes.

The QDIA closure is further discussed in the Appendix where the cumulant update QDIA (CUQDIA) closure, which has similar performance, but is more computationally efficient, is also described.

6. Topographic Rossby waves in a turbulent environment

Kasahara (1966) examined the generation of Rossby waves in numerical simulations of two-dimensional eastward and westward zonal flows impinging on isolated topography. He was able to explain much of the behaviour in his simulations and in earlier laboratory experiments by Fultz & Long (1951), and Fultz, Long & Frenzen (1955). Further contributions to the understanding of topographic Rossby wave generation were made in the numerical simulation studies of Egger (1970), Vergeiner & Ogura (1972), Edelmann (1972) and Grose & Hoskins (1979). Frederiksen (1982) compared linear steady-state theory with canonical equilibrium solutions while Verron & Le Provost (1985) studied quasi-geostrophic homogeneous flow impinging on isolated topography for both f - and β -planes.

In this section, we examine the generation of Rossby waves when eastward zonal currents impinge on a conical mountain in the presence of turbulence. We compare QDIA closure calculations with averages based on large ensembles of DNS for flow on the generalized β -plane. Here, we examine the accuracy of the QDIA closure in describing the evolution of topographic Rossby waves in four cases of medium to strong turbulence. In § 7, we consider atmospheric ensemble predictability in the case of strong mean flows and initial small-amplitude transient errors. Between them, our

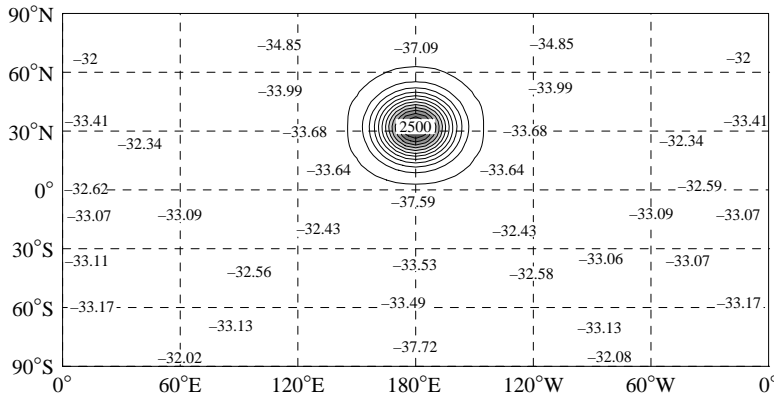


FIGURE 1. Circular conical mountain of height 2500 m centred at $30^\circ N$, $180^\circ W$ with a diameter of 45° latitude.

examples test the validity of the QDIA in describing Rossby wave turbulence for both strong and weak transients and strong and weak mean fields.

In this section and in §7, we use a length scale of $a/2$ and a time scale of Ω^{-1} ; the fields are mapped onto the doubly periodic domain, evolved and displayed on spherical projections. We examine the dynamics of Rossby waves for a β -effect of $1.15 \times 10^{-11} \text{ m}^{-1} \text{ s}^{-1}$ or a non-dimensional value of $\beta = 1/2$ and $k_0^2 = 1/2$ (typical of the β -effect at 60° latitude), and for a β -effect of $2.3 \times 10^{-11} \text{ m}^{-1} \text{ s}^{-1}$ or a non-dimensional value of $\beta = 1$ and $k_0^2 = 1$ (typical at the equator). Our experiments are carried out at circular $C16$ truncation for which $k \leq 16$ and this is adequate for our purposes since we focus on the dynamics of relatively large-scale Rossby waves. As in figure 4 of Frederiksen (1982), the conical mountain shown in our figure 1 is 2500 m high and is centred at $30^\circ N$, and $180^\circ W$ with a diameter of 45° latitude at the base.

6.1. Cases 1 and 2

For case 1, the initial large-scale flow U is eastward at 7.5 m s^{-1} (a non-dimensional value of 0.0325) and $\beta = 1/2$ and $k_0^2 = 1/2$, while for case 2 it is 15 m s^{-1} (a non-dimensional value of 0.065) and $\beta = 1$ and $k_0^2 = 1$. In these cases, the term $k_0^2 U$ makes only just over 3% or 6.5% contribution to the β -effect and we expect little quantitative difference between our results for the generalized β -plane and corresponding standard β -plane results. The results presented in this subsection are for dissipative flows with a viscosity of $2.5 \times 10^4 \text{ m}^2 \text{ s}^{-1}$ or a non-dimensional value of $\hat{\nu} = 3.378 \times 10^{-5}$.

The kinetic energy spectra of the initial transient and mean field contributions of the ‘small scales’ are as shown in figure 2(a) for case 1 and in figure 2(b) for case 2. The initial turbulent transients are Gaussian and isotropic and are several orders of magnitude larger than the mean field at all wavenumbers except for the large-scale mean field. Here, the band-averaged transient and mean kinetic energy spectra are defined as

$$E^T(k_i, t) = \frac{1}{2} \sum_{k \in S} [C_k(t, t)] / k^2, \quad (6.1a)$$

$$E^M(k_i, t) = \frac{1}{2} \sum_{k \in S} [\langle \zeta_k(t) \rangle \langle \zeta_{-k}(t) \rangle] / k^2. \quad (6.1b)$$

The set S is defined as

$$S = [\mathbf{k} | k_i = \text{Int.}[k + \frac{1}{2}]], \quad (6.2)$$

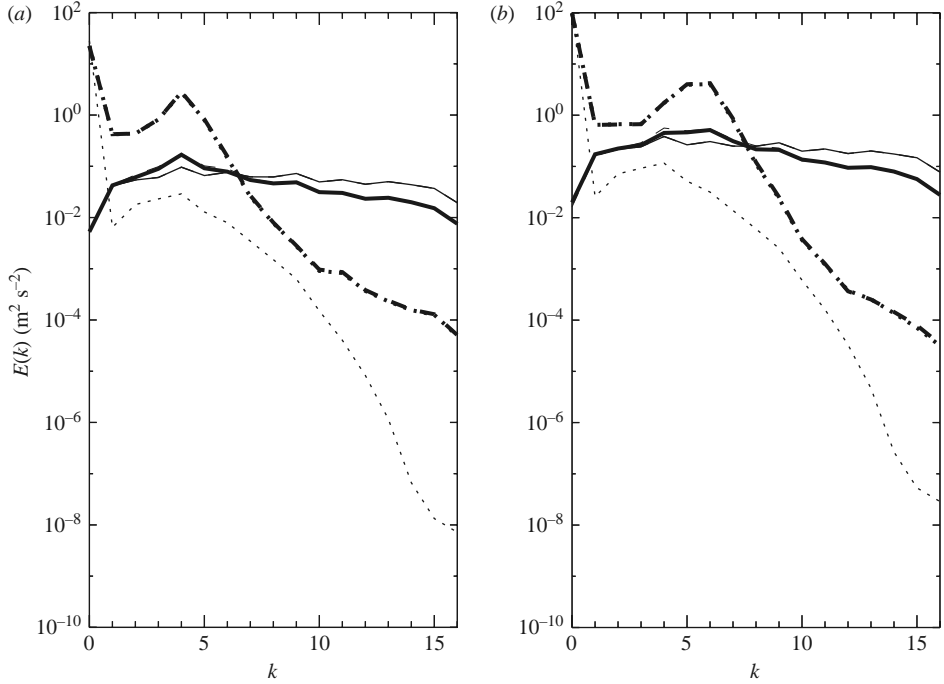


FIGURE 2. The evolved kinetic energy spectra in $\text{m}^2 \text{s}^{-2}$ for (a) case 1 and (b) case 2. Shown are: initial mean energy (thin dotted), initial transient energy (thin solid), evolved DNS mean energy (thick solid), evolved CUQDIA transient energy (thin dashed), evolved DNS mean energy (thick dotted) and evolved CUQDIA energy (thick dashed). Parameters used are given in table 1.

Case	Δt	\hat{v}	$C_k(0, 0)$	$\langle \zeta_k(0) \rangle$	a	b	U (m s^{-1})
1	0.21	3.378×10^{-5}	$\frac{0.01k^2}{a + bk^2}$	$-10bh_k C_k(0, 0)$	4.824×10^4	2.511×10^3	7.5
2	0.21	3.378×10^{-5}	$\frac{0.01k^2}{a + bk^2}$	$-10bh_k C_k(0, 0)$	4.824×10^4	2.511×10^3	15
3	0.21	3.378×10^{-5}	$\frac{k^2}{a + bk^2}$	$-bh_k C_k(0, 0)$	4.824×10^4	2.511×10^3	7.5
4	0.21	3.378×10^{-5}	$\frac{k^2}{a + bk^2}$	$-bh_k C_k(0, 0)$	4.824×10^4	2.511×10^3	15

TABLE 1. Parameters for figures 2–6.

where the subscript i indicates that the integer part is taken in (6.2) so that all k that lie within a given radius band of unit width are summed over. The kinetic energy of the large-scale flow is plotted at zero wavenumber.

The initial DNS fields have been constructed by first taking a Gaussian sample with zero mean and unit variance. For a given realization, we then obtain further members of the ensemble by moving its origin by an increment in the x -direction and then in the y -direction. The initial realization is moved successively by $2\pi/n$ in the x -direction to form n realizations. Each of these n realizations is then shifted by $2\pi/n$

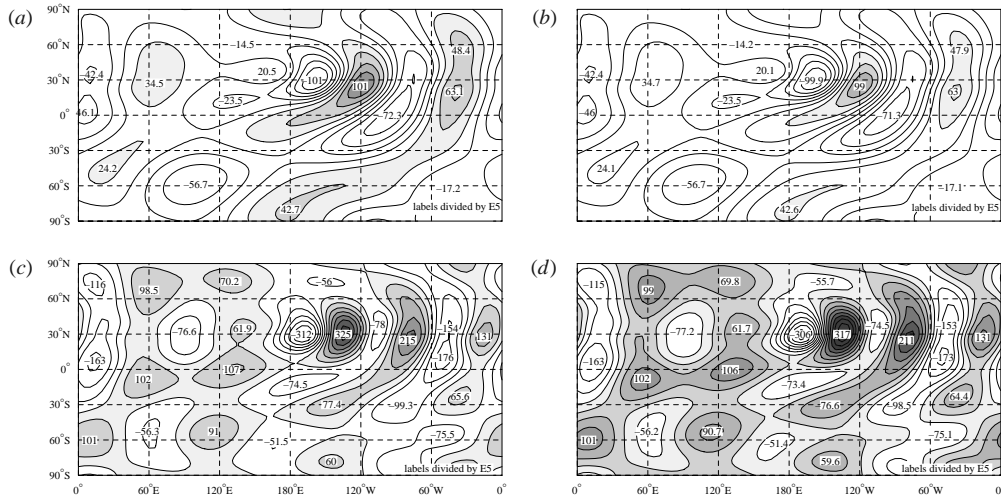


FIGURE 3. (a) The evolved day 10 DNS and (b) CUQDIA zonally asymmetric streamfunction in units of $10^5 \text{ m}^2 \text{ s}^{-1}$ for case 1. (c) The evolved day 10 DNS and (d) CUQDIA zonally asymmetric streamfunction for case 2.

in the y -direction to form a total of n^2 realizations. We then take the negative value of each of the n^2 elements so that we now have an ensemble of $2n^2$ realizations to which we give the required weights for the random and mean fields. The same process is then repeated with further initial Gaussian samples until an ensemble of the required number is obtained. This method ensures that not only are the initial fields accurate, but that the initial DNS covariance matrix is effectively isotropic for large enough n .

For both cases, the closure has been integrated forward for 10 days using the cumulant update restart procedure described in the Appendix. A time step of $1/30$ day, or a non-dimensional value of $\Delta t = 0.21$, was used and a restart carried out every day for the CUQDIA closure. For the DNS, 1800 realizations were integrated forward from the same initial mean and transient spectra as for the closure and again using a time step of $1/30$ day. Figure 2(a) also shows the evolved CUQDIA and ensemble-averaged DNS kinetic energy spectra on day 10 for case 1 and figure 2(b) shows case 2. In both the transient and mean components the evolved results for the DNS and closure are virtually indistinguishable. We see large increases in the mean field energies with peaks at wavenumber 4 for case 1 and at wavenumbers 5 and 6 for case 2 and a drop in the tail of the transient components.

The mean field peaks are a consequence of the topographic Rossby waves generated in the presence of differential rotation (Kasahara 1966; Frederiksen 1982; Verron & Le Provost 1985). Figure 3 shows the corresponding eddy, or zonally asymmetric, contribution to the streamfunction of the mean fields for both cases 1 and 2. These fields show the characteristic Rossby wave trains downstream of the conical mountain also seen in linear steady-state solutions (e.g. Figure 6 of Frederiksen 1982). The pattern correlation between the closure and DNS mean fields for the zonally asymmetric component of the streamfunction is 0.9999 in both cases, indicating the excellent agreement between closure and DNS results.

The contribution to the mean vorticity tendency from the transient eddies is given by the ensemble-average divergence of the eddy vorticity flux, $-\nabla \cdot \langle \hat{\mathbf{u}} \hat{\zeta} \rangle$, where $\hat{\mathbf{u}}$ is the wind, or equivalently $-\langle J(\hat{\psi}, \hat{\zeta}) \rangle$ while the corresponding contribution to the

mean streamfunction tendency is $-\nabla^{-2}\langle J(\hat{\psi}, \hat{\zeta}) \rangle \equiv -J^\psi$. As noted by Branstator & Frederiksen (2003) the streamfunction tendency due to transient eddies, $-J^\psi$, is an important diagnostic for understanding the role that transients play in the evolution of the mean fields. They showed, in a study of the observed climatological mean 300-hPa atmospheric streamfunction, that streamfunction tendencies are anticorrelated with the climatological zonally asymmetric mean in each month of the year. They also argued that this probably indicates that the transient perturbation structures that develop on a given mean state tend to be those that weaken the basic state eddies. It therefore seems of interest to compare the relationships between our mean zonally asymmetric streamfunctions in figure 3 and $-J^\psi$.

From (2.2) and (5.2b), we see that the Fourier transform of the streamfunction Jacobian J^ψ is given by

$$J_k^\psi(t) = -\frac{1}{k^2} \sum_p \sum_q \delta(\mathbf{k} + \mathbf{p} + \mathbf{q}) K(\mathbf{k}, \mathbf{p}, \mathbf{q}) C_{-p,-q}(t, t). \quad (6.3)$$

For the DNS, the streamfunction Jacobian $J_k^{\psi DNS}$ is calculated by generating the full covariance matrix and using the above expression. For the closure, $J_k^{\psi QDIA}$ can be further related to the nonlinear damping and eddy-topographic interaction through

$$\begin{aligned} J_k^{\psi QDIA}(t) &= -\frac{1}{k^2} \sum_p \sum_q \delta(\mathbf{k} + \mathbf{p} + \mathbf{q}) K(\mathbf{k}, \mathbf{p}, \mathbf{q}) C_{-p,-q}^{QDIA}(t, t) \\ &= -\frac{1}{k^2} \left\{ -\int_{t_0}^t ds \eta_k(t, s) \langle \zeta_k(s) \rangle + h_k \int_{t_0}^t ds \chi_k(t, s) \right. \\ &\quad \left. + \sum_p \sum_q \delta(\mathbf{k} + \mathbf{p} + \mathbf{q}) K(\mathbf{k}, \mathbf{p}, \mathbf{q}) \tilde{K}_{-p,-q}^{(2)}(t_0, t_0) R_{-p}(t, t_0) R_{-q}(t, t_0) \right\}, \quad (6.4) \end{aligned}$$

as seen from (5.2a) and (A 1). Here the nonlinear damping $\eta_k(t, s)$ is given in (A 2a) and eddy-topographic interaction $\chi_k(t, s)$ is given in (A 2b). It is clear from (6.4) that if the initial off-diagonal elements of the covariance are zero, ($\tilde{K}_{-p,-q}^{(2)}(t_0, t_0) = 0$), or small and the eddy-mean field interaction term $|\eta_k(t, s) \langle \zeta_k(s) \rangle|$ is significantly larger than the eddy-topographic interaction term $|\chi_k(t, s) h_k|$, then the streamfunction Jacobian is effectively a filtered version of the mean streamfunction. The streamfunction tendency $-J^\psi$ will therefore be anticorrelated with the mean streamfunction for (essentially) positive nonlinear damping. This argument appears to explain both the findings in the study of Branstator & Frederiksen (2003) and our results on the structure of the streamfunction tendency $-J^\psi$ that we consider next.

Figure 4 compares the evolved streamfunction tendency $-J^\psi$ on day 10 for the closure and DNS in cases 1 and 2 (for which $\tilde{K}_{-p,-q}^{(2)}(t_0, t_0) = 0$). For both cases, the comparison between closure and DNS Jacobians is quite good with a pattern correlation of 0.7419 in case 1 and of 0.7114 in case 2. As in the study of Branstator & Frederiksen (2003), the contribution to the streamfunction tendency owing to transient eddies, as measured by $-J^\psi$, is anticorrelated with the respective mean zonally asymmetric streamfunction fields in figure 3. Again the transient perturbations tend to weaken the mean state eddies.

6.2. Cases 3 and 4

For cases 3 and 4 we have repeated the same closure and DNS calculations as for cases 1 and 2 above, respectively, but with the initial transient kinetic energy

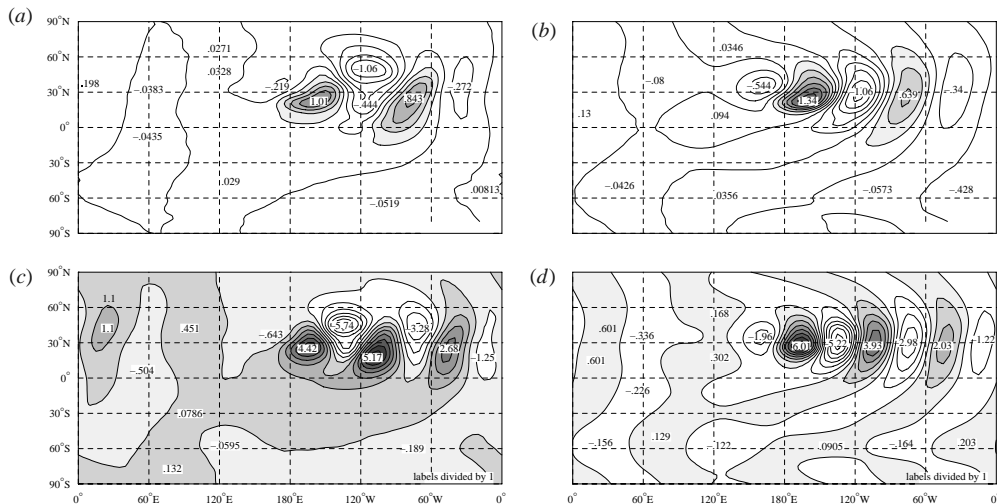


FIGURE 4. (a) The evolved day 10 DNS and (b) CUQDIA streamfunction tendency $-J^\psi$ in m^2s^{-2} for case 1. (c) The evolved day 10 DNS and (d) CUQDIA streamfunction tendency $-J^\psi$ for case 2.

spectrum increased by a factor of 100. We have calculated ensemble-averaged results based on both 800 and 1800 realizations of direct numerical simulations for case 3 and 1800 realizations for case 4. Our aim is to examine the sampling problem that may arise in calculating small-amplitude mean fields and spectra from ensemble-averaged DNS in the presence of strong turbulence (O’Kane & Frederiksen 2004).

For case 3, the initial and days 2 and 10 evolved energy spectra for the CUQDIA closure and DNS are shown in figure 5(a–c). We note from figure 5(b) that on day 2 there is close agreement between the closure and DNS mean energy spectra for $k < 12$, but at higher wavenumbers the DNS results overestimate the mean spectra, increasingly so for fewer realizations. Figure 5(c), which shows the evolved spectra on day 10, indicates that the DNS error in calculating the mean field increases with time and then saturates at a level depending on the number of realizations in the DNS ensemble. The results for case 4 on day 10, shown in figure 5(d), are very similar to those for case 3, but the transient energy spectrum is even stronger; the sampling error associated with the calculation of the ensemble-averaged mean spectrum is again evident. We also note that for ensembles of 100 to 200 realizations, the error in estimating the mean energy saturates at $\approx 1\%$ of the transient energy (not shown).

For case 3, figures 6(a) and 6(b) show the mean zonally asymmetric streamfunction for the DNS (based on 1800 realizations) and closure calculations on day 10. Despite the sampling problem resulting in some overestimation of DNS mean fields, the pattern correlation between DNS and closure results is 0.8974. For case 4 on day 10, the correspondence between DNS and closure mean fields (not shown) is closer, with a pattern correlation of 0.9726.

Figures 6(c) and 6(d) show the contribution to the mean streamfunction tendency owing to transient eddies for the DNS and closure in case 3. Again, $-J^\psi$ is anti-correlated with the mean zonally asymmetric streamfunction for both DNS and closure. The DNS and closure Jacobians have a pattern correlation of 0.8305, but

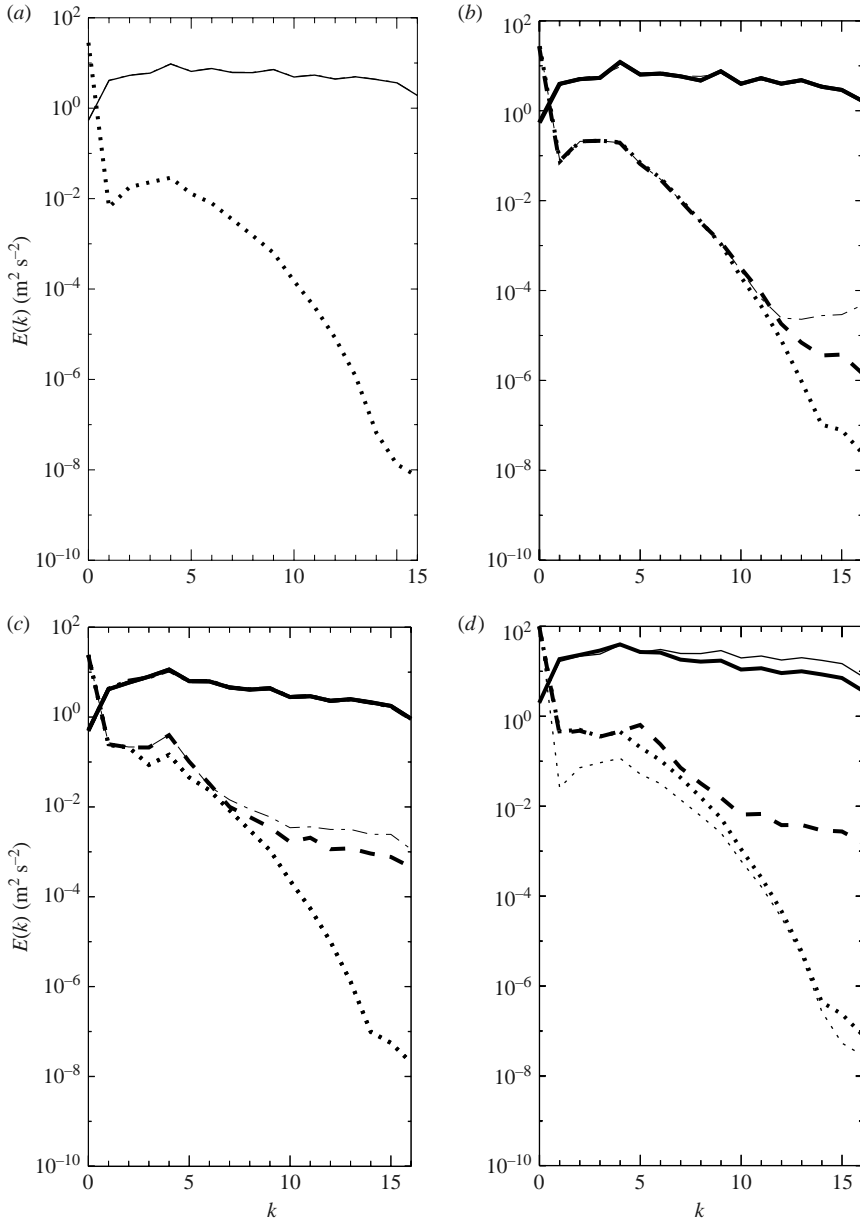


FIGURE 5. The evolved kinetic energy spectra ($\text{m}^2 \text{s}^{-2}$) at (a) 0, (b) 2 and (c) 10 days for case 3. (d) The evolved day 10 kinetic energy spectra for case 4. The line types are as described for figure 2(a–c). (d) The initial transient spectra is shown by a thin solid line and the initial mean field by a thin dotted line while the other spectral lines are as for (a–c). Parameters used are given in table 1.

it is also evident from figure 6(c) that the small-scale sampling errors of the DNS are reflected in the streamfunction tendency. Again, for case 4 on day 10, the DNS and closure Jacobians have a pattern correlation of 0.7407 and are structurally very similar to the respective results for case 3.

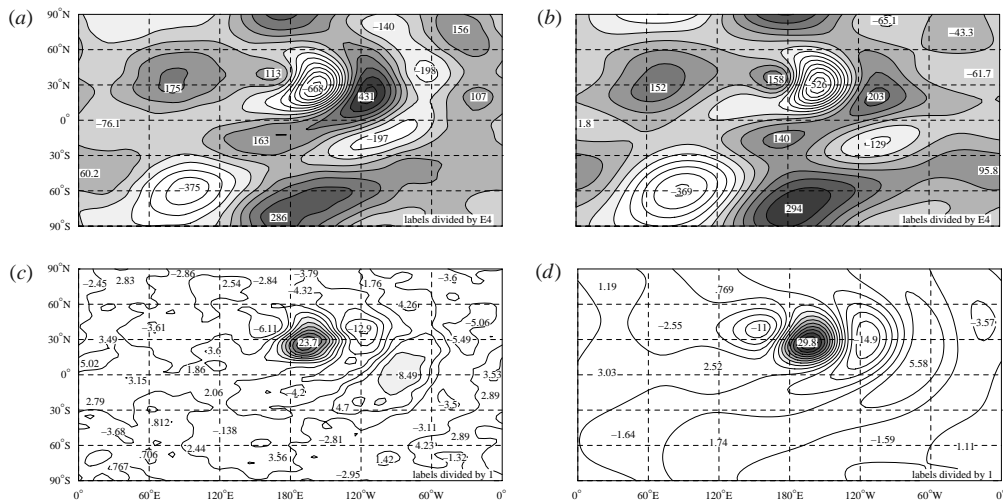


FIGURE 6. (a) The evolved day 10 DNS and (b) CUQDIA zonally asymmetric streamfunction (in $10^4 \text{ m}^2 \text{ s}^{-1}$) for case 3. (c) The evolved day 10 DNS and (d) CUQDIA streamfunction tendency $-J\psi$ ($\text{m}^2 \text{ s}^{-2}$) for case 3.

7. Ensemble predictability

The QDIA closure equations were derived based on the hypothesis that, to lowest order in perturbation theory, the covariance and response function matrices are diagonal. Frederiksen (1999) noted that sufficient conditions for this to occur are that the mean field and topography be small compared with the amplitudes of transients. However, these are not necessary conditions and it was pointed out that at canonical equilibrium, the off-diagonal elements of the equal time covariance matrix vanish, even for large mean field and topography. Indeed, the renormalization procedure removes divergences due to secular behaviour of the primitive perturbation theory and may enjoy some success outside the parameter regime where the primitive perturbation theory was formulated (Martin, Siggia & Rose 1972; Frederiksen & Davies 2000, 2004 and references therein).

Here, we examine the performance of the QDIA closure on the generalized β -plane when the initial mean field is of large amplitude compared with the transients and hence should provide a severe test of the closure. The situation that we consider is that of ensemble predictability where the mean field represents the ensemble mean forecast and the transients represent the error fields. We have considered this problem on both the f - and generalized β -planes, with the Doppler frequency treated perturbatively, and present results for $\beta = 1/2$ and $k_0^2 = 1/2$ and for a viscosity of $2.5 \times 10^5 \text{ m}^2 \text{ s}^{-1}$ corresponding to $\hat{\nu} = 3.378 \times 10^{-4}$.

We focus on the ensemble predictability of 500 hPa northern hemisphere atmospheric flows during a period in October and November 1979 that has been examined by Frederiksen, Collier & Watkins (2004) using two different general circulation models (GCMs). Our aim is not to try to reproduce the GCM results with a barotropic model, but rather to compare closure and ensemble-averaged DNS results for 10 day forecasts starting from an initial time that we chose to be 1200 UTC on 31 October 1979. During the subsequent period, a large-scale blocking high–low dipole formed over the Gulf of Alaska on 5 November, amplified and persisted until 12 November and then weakened and moved downstream (Frederiksen 1989). Figure 7(a) shows

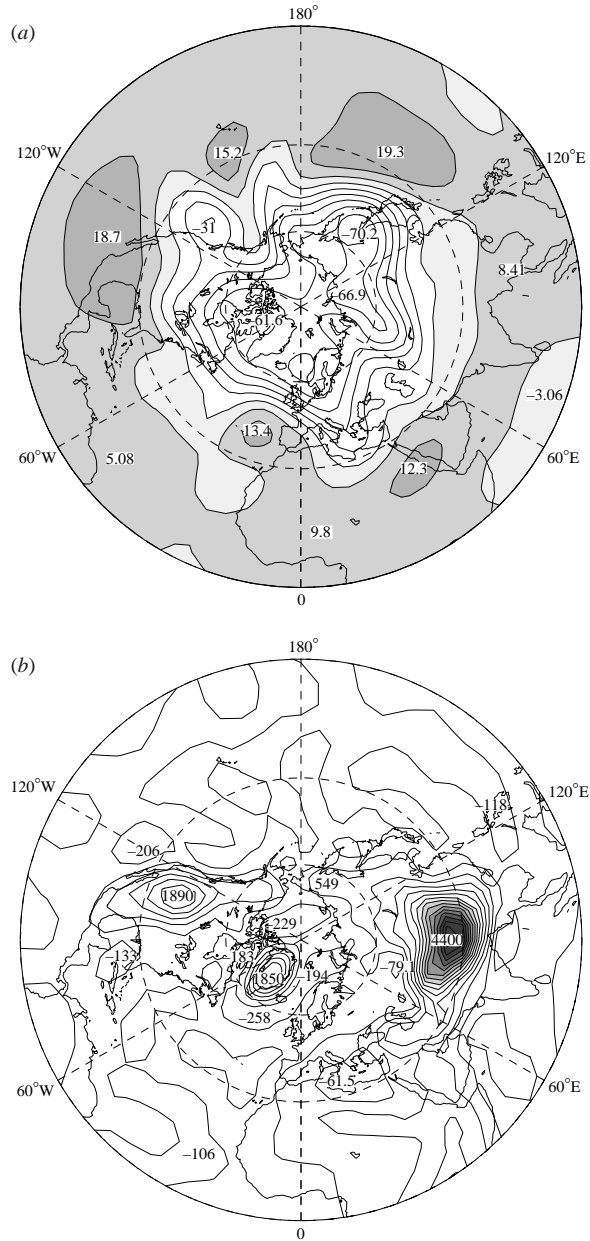


FIGURE 7. (a) 500 hPa streamfunction field at 1200 UTC on the 6 November 1979 in $\text{km}^2 \text{s}^{-1}$ and (b) northern hemisphere topography in m.

the 500 mb streamfunction field on 6 November 1979 when the block is developing while the northern hemisphere topography is shown in figure 7(b).

We examine the evolution of transient error fields in closure and DNS calculations on trajectories similar to that taken by the atmospheric 500 hPa field between 31 October and 9 November 1979. For the mean fields within a barotropic model to follow an observed trajectory closely, it is necessary to specify suitable time-evolving source terms. A relaxation term of the form

$$S_k(t) = \gamma(\zeta_k^* - \zeta_k) \quad (7.1)$$

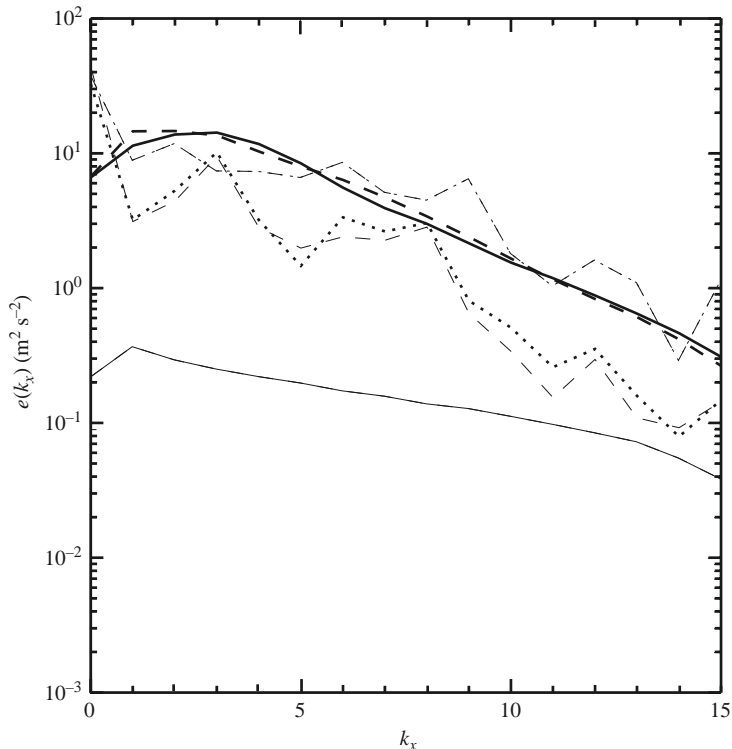


FIGURE 8. The evolved zonally averaged mean e^M and transient e^T kinetic energy spectra ($\text{m}^2 \text{s}^{-2}$) at the initial day and after 10 days of ensemble prediction for the β -plane case. Shown are: initial mean energy (thin dot-dashed), initial transient energy (thin solid), evolved DNS transient energy (thick solid), evolved CUQDIA transient energy (thick dashed), evolved CUQDIA mean energy (dotted) and evolved DNS mean energy (thin dashed).

is added to the right-hand side of (4.14) where ζ_k^* are the linearly interpolated daily observed fields. We start the simulation with the observed 500 hPa streamfunction for 1200 UTC on 31 October and use an e-folding relaxation time that varies from 2 days to 12 hours over a 5 day period and then remains at 12 hours for the last 5 days. The source term is calculated at each time step of the unperturbed simulation, stored and then applied to both perturbed ensemble DNS runs and to the mean field equation of the closure.

The initial errors fields have Gaussianly distributed isotropic spectra that are taken to be approximately constant with wavenumber k (apart from the zero component) as is characteristic of atmospheric kinetic energy error spectra (Molteni *et al.* 1996; Wei & Frederiksen 2004). For the DNS, we show the ensemble-average results from 1800 simulations; for both the closure and DNS, we use a time step of half an hour and for the CUQDIA closure a restart is performed every 2.5 days. Figure 8 shows the initial zonal wavenumber spectrum of the mean, e^M , and error, e^T , fields (truncated back to wavenumber 15) and also the corresponding day 10 evolved DNS and CUQDIA closure spectra. Here, $e^T(k_x, t)$ and $e^M(k_x, t)$ are defined by the right-hand sides of (6.1a) and (6.1b), but with the sums over k_y at the given k_x value. Throughout the 10 day forecast period, there is good agreement between the evolved DNS and closure mean spectra and, importantly, between the transient spectra as also shown in figure 8 on day 10.

8. Discussion and conclusions

We have developed the QDIA closure theory for the interaction of mean fields with Rossby waves and two-dimensional turbulence on a generalized β -plane. The generalized β -plane model for the barotropic-vorticity equation is in the same form as for the standard β -plane (Carnevale & Frederiksen 1987), but includes an extra term corresponding to the solid-body rotation vorticity on the sphere. This term makes a small, but structurally important, contribution to the planetary vorticity. The generalization has allowed us to establish a one-to-one correspondence between the dynamical equations and Rossby wave dispersion relations on the β -plane and on the sphere. We have formulated the nonlinear stability criteria for the stability of steady-state solutions, including the minimum enstrophy state, for inviscid unforced spectrally truncated flows over topography on the generalized β -plane. We have also presented the canonical equilibrium statistical mechanics on the generalized β -plane, discussed the relationships to nonlinear stability theory and to canonical equilibrium statistical mechanics theory on the sphere. As in the case of the standard β -plane (Carnevale & Frederiksen 1987), there is an equivalence between nonlinear stability theory and statistical mechanics in the limit of infinite resolution.

Importantly, generalizing the β -plane equations has allowed us to map the equations for the ‘small scales’ and for the large-scale flow U onto the standard f -plane form with generalized interaction coefficients and the large-scale flow appearing as a zero wavenumber field. The QDIA closure equations for the generalized β -plane then follow immediately from the argument of Frederiksen (1999) for the f -plane, but with the summations over wavenumbers also increased to include the zero wavenumber corresponding to the large-scale flow.

We have examined the performance of the QDIA closure, in cumulant update form, in comparison with the statistics of large ensembles of DNS at moderate resolution $k \leq 16$. Numerical experiments have been carried out to examine the generation of Rossby waves when eastward large-scale flows impinge on isolated topography in the presence of moderate to strong two-dimensional turbulence. Four cases have been presented with different strengths of the turbulent transients, β -effects and large-scale flows. For cases 1 and 2, with moderate strength of turbulent transients, the evolved transient and mean kinetic energy spectra for ensemble-averaged DNS based on 1800 realizations and the cumulant update QDIA closure are virtually identical out to day 10. The impact of the initial large-scale flow results in large increases in the mean field energy with peaks between wavenumber 4 and 6 associated with Rossby wave generation. These Rossby wavetrains are located downstream of the conical mountain as also seen in linear steady-state solutions (e.g. Frederiksen 1982) and the numerical studies of flow over isolated topography by Kasahara (1966) and Verron & Le Provost (1985). Again, there is excellent agreement between closure and DNS results, with pattern correlations between respective zonally asymmetric mean streamfunction fields of 0.9999 in both cases.

Cases 3 and 4 repeat experiments 1 and 2, respectively, but with 100 times the initial transient kinetic energy spectrum. With the stronger turbulent transients there are sampling errors in calculating the evolved DNS ensemble-averaged mean field, even with as many as 800 or 1800 realizations. The DNS mean spectral error, particularly at the smaller scales, increases with time and then saturates at a level depending on the number of realizations in the DNS ensemble, as in the case of f -plane topographic turbulence (O’Kane 2003; O’Kane & Frederiksen 2004). Despite this sampling problem in determining the DNS, zonally asymmetric mean streamfunction fields agree with pattern correlations of 0.8974 and 0.9726 for cases 3 and 4, respectively.

We have studied the role of the mean streamfunction tendency $-J^\psi$ contributed by the transient eddies in the development of the evolved zonally asymmetric mean streamfunction in the four cases. As in Branstator & Frederiksen (2003), the streamfunction tendency $-J^\psi$ is anticorrelated with the zonally asymmetric mean streamfunction for both the DNS and closure. Pattern correlations between DNS and closure Jacobians range from larger than 0.7 to larger than 0.8 in the four cases, also indicating quite good comparison for this diagnostic. On the basis of the QDIA closure expression for $-J^\psi$ in terms of products of nonlinear damping and mean field and of eddy-topographic interaction and topography, we have provided a theoretical explanation for our findings and for those of Branstator & Frederiksen (2003). Again, it appears that the transient perturbation structures that evolve on a given mean state tend to be those that weaken the basic-state eddies.

Finally, we have studied the performance of the QDIA closure both on the generalized β -plane when the initial mean field is of large amplitude compared with the transients. This has provided a severe test of the closure since it was founded on the basis that to lowest order in perturbation theory, the covariance and response functions are diagonal. The particular situation we have considered is that of ensemble predictability of northern hemisphere flows in 10 day forecasts starting from 31 of October 1979 in which the mean field represents the ensemble mean forecast and the transients are the error fields which are initially isotropic. We have found that on both the f -plane (not shown) and generalized β -plane there is agreement between the evolved DNS and closure mean spectra for periods out to 10 days. As well there are close similarities between the transient DNS and closure spectra in these 10 day simulations.

In summary, the QDIA closure, as employed here in cumulant update form, is in general in very good agreement with the statistics of DNS where sampling problems do not affect the DNS results. In future works, we hope to apply the QDIA closure to problems in atmospheric and geophysical fluid dynamics, to regime transitions and ensemble prediction (e.g. Frederiksen *et al.* 2004 and references therein) and to subgrid scale parameterizations (e.g. Frederiksen 1999 and references therein). In studies at higher resolution, we expect that it will be necessary to also employ the regularization method (Frederiksen & Davies 2004; O’Kane & Frederiksen 2004) briefly discussed in the Appendix in order to obtain accurate small-scale spectra for the closure.

Appendix. The cumulant update QDIA closure on a β -plane

Here we further discuss the QDIA closure equations on the generalized β -plane including a more efficient version termed the cumulant update QDIA (CUQDIA). The mean-field equation can be written in the form

$$\begin{aligned}
 \left(\frac{\partial}{\partial t} + \nu_0(\mathbf{k})k^2\right)\langle\zeta_{\mathbf{k}}\rangle &= \sum_{\mathbf{p}} \sum_{\mathbf{q}} \delta(\mathbf{k} + \mathbf{p} + \mathbf{q}) [K(\mathbf{k}, \mathbf{p}, \mathbf{q})\langle\zeta_{-\mathbf{p}}(t)\rangle\langle\zeta_{-\mathbf{q}}(t)\rangle \\
 &\quad + A(\mathbf{k}, \mathbf{p}, \mathbf{q})\langle\zeta_{-\mathbf{p}}(t)\rangle h_{-\mathbf{q}}] - \int_{t_0}^t ds \eta_{\mathbf{k}}(t, s)\langle\zeta_{\mathbf{k}}(s)\rangle \\
 &\quad + h_{\mathbf{k}} \int_{t_0}^t ds \chi_{\mathbf{k}}(t, s) + \langle f_{\mathbf{k}}^0(t)\rangle \\
 &\quad + \sum_{\mathbf{p}} \sum_{\mathbf{q}} \delta(\mathbf{k} + \mathbf{p} + \mathbf{q}) K(\mathbf{k}, \mathbf{p}, \mathbf{q}) \tilde{K}_{-\mathbf{p}, -\mathbf{q}}^{(2)}(t_0, t_0) R_{-\mathbf{p}}(t, t_0) R_{-\mathbf{q}}(t, t_0).
 \end{aligned}
 \tag{A 1}$$

Here, the nonlinear damping

$$\eta_k(t, s) = -4 \sum_p \sum_q \delta(\mathbf{k} + \mathbf{p} + \mathbf{q}) K(\mathbf{k}, \mathbf{p}, \mathbf{q}) K(-\mathbf{p}, -\mathbf{q}, -\mathbf{k}) R_{-p}(t, s) C_{-q}(t, s), \quad (\text{A } 2a)$$

measures the interaction of transient eddies with the mean field while

$$\chi_k(t, s) = 2 \sum_p \sum_q \delta(\mathbf{k} + \mathbf{p} + \mathbf{q}) K(\mathbf{k}, \mathbf{p}, \mathbf{q}) A(-\mathbf{p}, -\mathbf{q}, -\mathbf{k}) R_{-p}(t, s) C_{-q}(t, s), \quad (\text{A } 2b)$$

measures the strength of the interaction of transient eddies with the topography.

Equation (5.8) for the diagonal two-time two-point cumulant can be rewritten in the form:

$$\left(\frac{\partial}{\partial t} + \nu_0(\mathbf{k}) k^2 \right) C_k(t, t') = N_k(t, t'), \quad (\text{A } 3)$$

where

$$\begin{aligned} N_k(t, t') &= \int_{t_0}^{t'} ds [S_k(t, s) + P_k(t, s) + F_k^0(t, s)] R_{-k}(t', s) \\ &\quad - \int_{t_0}^t ds [\eta_k(t, s) + \pi_k(t, s)] C_{-k}(t', s) + \sum_p \sum_q \delta(\mathbf{k} + \mathbf{p} + \mathbf{q}) \\ &\quad \times K(\mathbf{k}, \mathbf{p}, \mathbf{q}) \tilde{K}_{-q, -p, -k}^{(3)}(t_0, t_0, t_0) R_{-q}(t, t_0) R_{-p}(t, t_0) R_{-k}(t', t_0) \\ &\quad + \sum_p \sum_q \delta(\mathbf{k} + \mathbf{p} + \mathbf{q}) [K(\mathbf{k}, \mathbf{p}, \mathbf{q}) \langle \zeta_{-q}(t) \rangle + A(\mathbf{k}, \mathbf{p}, \mathbf{q}) h_{-q}] \\ &\quad \times \tilde{K}_{-p, -k}^{(2)}(t_0, t_0) R_{-p}(t, t_0) R_{-k}(t', t_0). \end{aligned} \quad (\text{A } 4)$$

Here,

$$F_k^0(t, s) = \langle \hat{f}_k^0(t) \hat{f}_k^{0*}(s) \rangle \quad (\text{A } 5a)$$

is the variance of the random forcing,

$$S_k(t, s) = 2 \sum_p \sum_q \delta(\mathbf{k} + \mathbf{p} + \mathbf{q}) K(\mathbf{k}, \mathbf{p}, \mathbf{q}) K(-\mathbf{k}, -\mathbf{p}, -\mathbf{q}) C_{-p}(t, s) C_{-q}(t, s), \quad (\text{A } 5b)$$

is the nonlinear noise and

$$\begin{aligned} P_k(t, s) &= \sum_p \sum_q \delta(\mathbf{k} + \mathbf{p} + \mathbf{q}) C_{-p}(t, s) [K(\mathbf{k}, \mathbf{p}, \mathbf{q}) \langle \zeta_{-q}(t) \rangle + A(\mathbf{k}, \mathbf{p}, \mathbf{q}) h_{-q}] \\ &\quad \times [K(-\mathbf{k}, -\mathbf{p}, -\mathbf{q}) \langle \zeta_q(s) \rangle + A(-\mathbf{k}, -\mathbf{p}, -\mathbf{q}) h_q], \end{aligned} \quad (\text{A } 5c)$$

$$\begin{aligned} \pi_k(t, s) &= - \sum_p \sum_q \delta(\mathbf{k} + \mathbf{p} + \mathbf{q}) R_{-p}(t, s) [K(\mathbf{k}, \mathbf{p}, \mathbf{q}) \langle \zeta_{-q}(t) \rangle + A(\mathbf{k}, \mathbf{p}, \mathbf{q}) h_{-q}] \\ &\quad \times [K(-\mathbf{p}, -\mathbf{k}, -\mathbf{q}) \langle \zeta_q(s) \rangle + A(-\mathbf{p}, -\mathbf{k}, -\mathbf{q}) h_q], \end{aligned} \quad (\text{A } 5d)$$

are noise and dissipation terms associated with eddy–mean field and eddy–topographic interactions. Equations (A 1), (A 3) and (A 4) generalize the QDIA closure of Frederiksen (1999) by including initial contributions to the off-diagonal covariance matrix ($\tilde{K}_{-p, -k}^{(2)}(t_0, t_0)$) and to non-Gaussian initial conditions associated with the three-point function ($\tilde{K}_{-q, -p, -k}^{(3)}(t_0, t_0, t_0)$).

Equation (5.9) for the diagonal response function can be rewritten in the form:

$$\left(\frac{\partial}{\partial t} + v_0(\mathbf{k})k^2\right)R_k(t, t') = - \int_{t'}^t ds [\eta_k(t, s) + \pi_k(t, s)]R_k(s, t'), \quad (\text{A } 6)$$

with $R_k(t, t) = 1$ and for $t < t'$ we have $R_k(t, t') = 0$. The equation for the diagonal single-time two-point cumulant is

$$\left(\frac{\partial}{\partial t} + 2Re v_0(\mathbf{k})k^2\right)C_k(t, t) = 2Re N_k(t, t) \quad (\text{A } 7a)$$

since

$$\frac{\partial C_k(t, t)}{\partial t} = \lim_{t' \rightarrow t} \left(\frac{\partial C_k(t, t')}{\partial t} + \frac{\partial C_k(t, t')}{\partial t'} \right), \quad (\text{A } 7b)$$

and $C_k(t', t) = C_{-k}(t, t') = C_k^*(t, t')$.

These QDIA closure equations, including off-diagonal and non-Gaussian initial conditions may then be used to periodically truncate the potentially long time-history integrals (Rose 1985; Frederiksen, Davies & Bell 1994) and obtain a more efficient closure scheme which we call the cumulant update QDIA (CUQDIA, O'Kane 2003; O'Kane & Frederiksen 2004). The method relies on the fact that the essential information contained in the time-history integrals is the off-diagonal two-point cumulant and the three-point cumulant. Suppose we integrate the QDIA closure equations from the initial time $t_0 = 0$ up to a time $t' = t = T$. Then, the off-diagonal two-point cumulant and the three-point cumulant may be calculated through the relationships

$$\tilde{K}_{-p, -k}^{(2)}(T, T) = K_{-p, -k}^{(2)Dyn}(T, T) + \tilde{K}_{-p, -k}^{(2)}(t_0, t_0)R_{-p}(T, t_0)R_{-k}(T, t_0), \quad (\text{A } 8a)$$

$$\begin{aligned} \tilde{K}_{-q, -p, -k}^{(3)}(T, T, T) &= K_{-q, -p, -k}^{(3)Dyn}(T, T, T) \\ &+ \tilde{K}_{-q, -p, -k}^{(3)}(t_0, t_0, t_0)R_{-q}(T, t_0)R_{-p}(T, t_0)R_{-k}(T, t_0). \end{aligned} \quad (\text{A } 8b)$$

Here

$$\begin{aligned} K_{-p, -k}^{(2)Dyn}(t, t') &= \int_{t_0}^t ds R_{-p}(t, s)C_{-k}(t', s) \\ &\times [A(-\mathbf{p}, -\mathbf{k}, \mathbf{k} + \mathbf{p})h_{(-k-p)} + K(-\mathbf{p}, -\mathbf{k}, \mathbf{k} + \mathbf{p})\langle \zeta_{(-k-p)}(s) \rangle] \\ &+ \int_{t_0}^{t'} ds R_{-k}(t', s)C_{-p}(t, s) \\ &\times [A(-\mathbf{k}, -\mathbf{p}, \mathbf{k} + \mathbf{p})h_{(-k-p)} + K(-\mathbf{k}, -\mathbf{p}, \mathbf{k} + \mathbf{p})\langle \zeta_{(-k-p)}(s) \rangle], \end{aligned} \quad (\text{A } 9a)$$

and

$$\begin{aligned} K_{-q, -p, -k}^{(3)Dyn}(t, t, t') &= 2 \int_{t_0}^{t'} ds K(-\mathbf{k}, -\mathbf{p}, -\mathbf{q})C_{-q}(t, s)C_{-p}(t, s)R_{-k}(t', s) \\ &+ 2 \int_{t_0}^{t'} ds K(-\mathbf{q}, -\mathbf{k}, -\mathbf{p})R_{-q}(t, s)C_{-p}(t, s)C_{-k}(t', s) \\ &+ 2 \int_{t_0}^{t'} ds K(-\mathbf{p}, -\mathbf{q}, -\mathbf{k})R_{-p}(t, s)C_{-q}(t, s)C_{-k}(t', s). \end{aligned} \quad (\text{A } 9b)$$

Equations (A 8) and (A 9) follow from consistency with (A 1), (A 3) and (A 4). The procedure may then be performed as often as required by simply replacing

$\tilde{K}_{-p,-k}^{(2)}(t_0, t_0)$, $\tilde{K}_{-p,-q}^{(2)}(t_0, t_0)$ and $\tilde{K}_{-q,-p,-k}^{(3)}(t_0, t_0, t_0)$ with the quantities $\tilde{K}_{-p,-k}^{(2)}(T, T)$, $\tilde{K}_{-p,-q}^{(2)}(T, T)$ and $\tilde{K}_{-q,-p,-k}^{(3)}(T, T, T)$.

The DIA (Kraichnan 1958, 1959a) and QDIA (Frederiksen 1999) closures do not distinguish between convection effects and intrinsic distortion effects. This leads to power laws at high resolution and Reynolds numbers that differ slightly from the Kolmogorov inertial range power laws (Kraichnan 1964c). A way of overcoming this is to zero the interaction coefficients if $p < k/\alpha$ or $q < k/\alpha$ in the two-time cumulant and response function equations of the closures where α is an empirically determined parameter (Kraichnan 1964c; Kadomtsev 1965; Sudan & Pfirsch 1985; Frederiksen & Davies 2004; O'Kane & Frederiksen 2004). This same method may also be used for the QDIA closure on the generalized β -plane.

REFERENCES

- ABRAMOV, R. V. & MAJDA, A. J. 2003 Statistically relevant conserved quantities for truncated quasi-geostrophic flow. *Proc. Natl Acad. Sci.* **100**, 3841–3846.
- ALVAREZ, A., TINTORE, J., HOLLOWAY, G., EBY, M. & BECKERS, J. M. 1994 Effect of topographic stress on circulation in the western Mediterranean. *J. Geophys. Res.* **99**, 16 053–16 064.
- ARNOLD, V. I. 1965 On conditions for nonlinear stability of plane stationary curvilinear flows of an ideal fluid. *Sov. Math. Dokl.* **6**, 773–777.
- BOWMAN, J. C. & KROMMES, J. A. 1997 The realizable Markovian closure and realizable test-field model II. Application to anisotropic drift-wave dynamics. *Phys. Plasmas* **4**, 3895–3909.
- BOWMAN, J. C., KROMMES, J. A. & OTTAVIANI, M. 1993 The realizable Markovian closure I. General theory, with applications to 3-wave dynamics. *Phys. Fluids* **5**, 3558–3589.
- BRANSTATOR, G. & FREDERIKSEN, J. 2003 The seasonal cycle of interannual variability and the dynamical imprint of the seasonally varying mean state. *J. Atmos. Sci.* **60**, 1577–1592.
- CARNEVALE, G. F. & FREDERIKSEN, J. S. 1987 Nonlinear stability and statistical mechanics of flow over topography. *J. Fluid Mech.* **175**, 157–181.
- CARNEVALE, G. F., PURINI, R., ORLANDI, P. & CAVAZZA, P. 1995 Barotropic quasi-geostrophic f -plane flow over anisotropic topography. *J. Fluid Mech.* **285**, 329–347.
- CHASNOV, J. R. 1991 Simulation of the Kolmogorov inertial subrange using an improved subgrid model. *Phys. Fluids A* **3**, 188–200.
- CHAVANIS, P. H. & SOMMERIA, J. 2002 Statistical mechanics of the shallow water system. *Phys. Rev. E* **65**, 026302:1–13.
- DEKER, U. & HAAKE, F. 1975 Fluctuation–dissipation theorems for classical processes. *Phys. Rev. A* **6**, 2043–2056.
- EGGER, J. 1970 On the simulation of subgrid orographic effects in numerical forecasting. *J. Atmos. Sci.* **27**, 896–902.
- EDELMANN, W. 1972 Numerical experiments with a barotropic current across mountains. *Beitr. Z. Phys. Atmos.* **45**, 196–229.
- ELLIS, R. S., HAVEN, K. & TURKINGTON, B. 2002 Nonequivalent statistical equilibrium ensembles and refined stability theorems for most probable flows. *Nonlinearity* **15**, 239–255.
- FREDERIKSEN, C. S. & FREDERIKSEN, J. S. 1989 Flow over topography and instability on beta-planes: the effects of different expansion representations. *J. Atmos. Sci.* **46**, 1664–1686.
- FREDERIKSEN, C. S. & FREDERIKSEN, J. S. 1991 Flow over topography and instability on a sphere. *J. Atmos. Sci.* **48**, 2411–2425.
- FREDERIKSEN, J. S. 1982 Eastward and westward flows over topography in nonlinear and linear barotropic models. *J. Atmos. Sci.* **39**, 2477–2489.
- FREDERIKSEN, J. S. 1989 The role of instability during the onset of blocking and cyclogenesis in Northern Hemisphere synoptic flows. *J. Atmos. Sci.* **46**, 1076–1092.
- FREDERIKSEN, J. S. 1999 Subgrid-scale parameterizations of eddy-topographic force, eddy viscosity, and stochastic backscatter for flow over topography. *J. Atmos. Sci.* **56**, 1481–1494.
- FREDERIKSEN, J. S. & CARNEVALE, G. F. 1986 Stability properties of exact nonzonal solutions for flow over topography. *Geophys. Astrophys. Fluid Dyn.* **35**, 173–207.

- FREDERIKSEN, J. S., COLLIER, M. A. & WATKINS, A. B. 2004 Ensemble prediction of blocking regime transitions. *Tellus* **56** A, 485–500.
- FREDERIKSEN, J. S. & DAVIES, A. G. 1997 Eddy viscosity and stochastic backscatter parameterizations on the sphere for atmospheric circulation models. *J. Atmos. Sci.* **54**, 2475–2492.
- FREDERIKSEN, J. S. & DAVIES, A. G. 2000 Dynamics and spectra of cumulant update closures for two-dimensional turbulence. *Geophys. Astrophys. Fluid Dyn.* **92**, 197–231.
- FREDERIKSEN, J. S. & DAVIES, A. G. 2004 The regularized DIA closure for two-dimensional turbulence. *Geophys. Astrophys. Fluid Dyn.* **98**, 203–223.
- FREDERIKSEN, J. S., DAVIES, A. G. & BELL, R. C. 1994 Closure equations with non-Gaussian restarts for truncated two-dimensional turbulence. *Phys. Fluids* **6**, 3153–3163.
- FREDERIKSEN, J. S., DIX, M. R. & DAVIES, A. G. 2003 The effects of closure-based eddy diffusion on the climate and spectra of a GCM. *Tellus* **55** A, 31–44.
- FREDERIKSEN, J. S. & SAWFORD, B. L. 1981 Topographic waves in nonlinear and linear spherical barotropic models. *J. Atmos. Sci.* **38**, 69–86.
- FULTZ, D. & LONG, R. R. 1951 Two-dimensional flow around a circular barrier in a rotating spherical shell. *Tellus* **3**, 61–68.
- FULTZ, D., LONG, R. R. & FRENZEN, P. 1955 A note on certain interesting ageostrophic motions in a rotating hemispherical shell. *J. Met.* **12**, 323–338.
- GROSE, W. L. & HOSKINS, B. J. 1979 On the influence of orography on large-scale atmospheric flow. *J. Atmos. Sci.* **36**, 223–234.
- HERRING, J. R. 1965 Self-consistent-field approach to turbulence theory. *Phys. Fluids* **8**, 2219–2225.
- HERRING, J. R. 1977 On the statistical theory of two-dimensional topographic turbulence. *J. Atmos. Sci.* **34**, 1731–1750.
- HERRING, J. R. 1983 The predictability of quasi-geostrophic flows. *Proc. AIP Conf. No. 106, Predictability of Fluid Motions* (ed. G. Holloway & B. J. West), pp. 67–77.
- HERRING, J. R., ORSZAG, S. A., KRAICHNAN, R. H. & FOX, D. G. 1974 Decay of two-dimensional homogeneous turbulence. *J. Fluid Mech.* **66**, 417–444.
- HOLLOWAY, G. 1978 A spectral theory of nonlinear barotropic motion above irregular topography. *J. Phys. Oceanogr.* **8**, 414–427.
- HOLLOWAY, G. 1987 Systematic forcing of large-scale geophysical flows by eddy–topographic interaction. *J. Fluid Mech.* **184**, 463–476.
- HOLLOWAY, G. 1992 Representing topographic stress for large-scale ocean models. *J. Phys. Oceanogr.* **22**, 1033–1046.
- ISICHENKO, M. B. & GRUZINOV, A. V. 1994 Coherent structures, and Gaussian turbulence in 2-dimensional (2-D) magnetohydrodynamics (MHD). *Phys. Plasmas* **1**, 1802–1816.
- KADOMTSEV, B. B. 1965 *Plasma Turbulence*. Academic.
- KASAHARA, A. 1966 The dynamical influence of orography on the large scale motion of the atmosphere. *J. Atmos. Sci.* **23**, 259–270.
- KAZANTSEV, E., SOMMERIA, J. & VERRON, J. 1998 Subgrid-scale eddy parameterization by statistical mechanics in a barotropic ocean model. *J. Phys. Oceanogr.* **28**, 1017–1042.
- KRAICHNAN, R. H. 1958 Irreversible statistical mechanics of incompressible hydrodynamic turbulence. *Phys. Rev.* **109**, 1407–1422.
- KRAICHNAN, R. H. 1959a The structure of isotropic turbulence at very high Reynolds numbers. *J. Fluid Mech.* **5**, 497–543.
- KRAICHNAN, R. H. 1959b Classical fluctuation-relaxation theorem. *Phys. Rev.* **113**, 1181–1182.
- KRAICHNAN, R. H. 1964a Decay of isotropic turbulence in the direct interaction approximation. *Phys. Fluids* **7**, 1030–1048.
- KRAICHNAN, R. H. 1964b Diagonalizing approximation for inhomogeneous turbulence. *Phys. Fluids* **7**, 1169–1177.
- KRAICHNAN, R. H. 1964c Kolmogorov’s hypothesis and Eulerian turbulence theory. *Phys. Fluids* **7**, 1723–1734.
- KRAICHNAN, R. H. 1970 Instability in fully developed turbulence. *Phys. Fluids* **13**, 569–575.
- KRAICHNAN, R. H. 1971a An almost-Markovian Galilean-invariant turbulence model. *J. Fluid Mech.* **47**, 513–524.
- KRAICHNAN, R. H. 1971b Inertial-range transfer in two- and three-dimensional turbulence. *J. Fluid Mech.* **47**, 525–535.

- KRAICHNAN, R. H. 1972 Test-field model for inhomogeneous turbulence. *J. Fluid Mech.* **56**, 287–304.
- KRAICHNAN, R. H. 1976 Eddy viscosity in two and three dimensions. *J. Atmos. Sci.* **33**, 1521–1536.
- KRAICHNAN, R. H. & HERRING, J. R. 1978 A strain-based Lagrangian-history turbulence theory. *J. Atmos. Sci.* **88**, 355–367.
- LEITH, C. E. 1971 Atmospheric predictability and two-dimensional turbulence. *J. Atmos. Sci.* **28**, 145–161.
- LEITH, C. E. 1974 Theoretical skill of Monte Carlo forecasts. *Mon. Weather Rev.* **102**, 409–418.
- LEITH, C. E. 1975 Climate response and fluctuation dissipation. *J. Atmos. Sci.* **32**, 2022–2027.
- LEITH, C. E. 1990 Stochastic backscatter in a subgrid-scale model: plane shear mixing layer. *Phys. Fluids A* **2**, 297–299.
- LEITH, C. E. & KRAICHNAN, R. H. 1972 Predictability of turbulent flows. *J. Atmos. Sci.* **29**, 1041–1058.
- MCCOMB, W. D. 1974 A local energy-transfer theory of isotropic turbulence. *J. Phys. A* **7**, 632–649.
- MCCOMB, W. D. 1990 *The Physics of Fluid Turbulence*. Clarendon.
- MCCOMB, W. D., FILIPIAK, M. J. & SHANMUGASUNDARAM, V. 1992 Rederivation and further assessment of the LET theory of isotropic turbulence, as applied to passive scalar convection. *J. Fluid Mech.* **245**, 279–300.
- MCCOMB, W. D. & QUINN, A. P. 2003 Two-point two-time closures applied to forced isotropic turbulence. *Physica A* **317**, 487–508.
- MAJDA, A. J. & HOLEN, M. 1997 Dissipation, topography, and statistical theories for large-scale coherent structure. *Commun. Pure Appl. Maths* **50**, 1183–1234.
- MARTIN, P. C., SIGGIA, E. D. & ROSE, H. A. 1973 Statistical dynamics of classical systems. *Phys. Rev. A* **8**, 423–437.
- MERRYFIELD, W. J. & HOLLOWAY, G. 1997 Topographic stress parameterization in a quasi-geostrophic barotropic model. *J. Fluid Mech.* **341**, 1–18.
- MERRYFIELD, W. J. & HOLLOWAY, G. 2002 Predictability of quasi-geostrophic turbulence. *J. Fluid Mech.* **465**, 191–212.
- MERRYFIELD, W. J., CUMMINS, P. F. & HOLLOWAY, G. 2001 Equilibrium statistical mechanics of barotropic flow over finite topography. *J. Phys. Oceanogr.* **31**, 1880–1890.
- MÉTAIS, O. & LESIEUR, M. 1986 Statistical predictability of decaying turbulence. *J. Atmos. Sci.* **43**, 857–870.
- MILLER, J., WEICHMAN, P. B. & CROSS, M. C. 1992 Statistical mechanics, Euler equation, and Jupiter's red spot. *Phys. Rev. A* **45**, 2328–2359.
- MOLTENI, F., BUIZZA, R., PALMER, T. & PETROLIAGIS, T. 1996 The ECMWF ensemble prediction system: methodology and validation. *Q. J. Met. Soc.* **122**, 73–119.
- O'KANE, T. J. 2003 The statistical dynamics of geophysical flows: An investigation of two-dimensional turbulent flow over topography. PhD thesis, Monash University, Australia.
- O'KANE, T. J. & FREDERIKSEN, J. S. 2004 The QDIA and regularized QDIA closures for inhomogeneous turbulence over topography. *J. Fluid Mech.* **504**, 133–165.
- ORSZAG, S. A. 1970 Analytical theories of turbulence. *J. Fluid Mech.* **41**, 363–386.
- POLYAKOV, I. 2001 An eddy parameterization based on maximum entropy production with application to modelling of the Arctic ocean circulation. *J. Phys. Oceanogr.* **31**, 2255–2270.
- POUQUET, A., LESIEUR, M., ANDRÉ, J. C. & BASDEVANT, C. 1975 Evolution of high Reynolds number two-dimensional turbulence. *J. Fluid Mech.* **72**, 305–319.
- ROSE, H. A. 1977 Eddy diffusivity, eddy noise and subgrid-scale modelling. *J. Fluid Mech.* **81**, 719–734.
- ROSE, H. A. 1985 An efficient non-Markovian theory of non-equilibrium dynamics. *Physica D* **14**, 216–226.
- SALMON, R., HOLLOWAY, G. & HENDERSHOTT, M. C. 1976 The equilibrium statistical mechanics of simple quasi-geostrophic models. *J. Fluid Mech.* **75**, 691–703.
- SCHILLING, O. & ZHOU, Y. 2002 Analysis of spectral eddy viscosity and backscatter in incompressible, isotropic turbulence using statistical closure theory. *Phys. Fluids* **14**, 1244–1258.
- SUDAN, R. N. & PFIRSCH, D. 1985 On the relation between 'mixing length' and 'direct interaction approximation' theories of turbulence. *Phys. Fluids* **28**, 1702–1718.

- TURKINGTON, B., MAJDA, A., HAVEN, K. & DiBATTISTA, M. 2001 Statistical equilibrium predictions of jets and spots on Jupiter. *Proc. Natl Acad. Sci.* **98**, 12 346–12 350.
- VERGEINER, I. & OGURA, Y. 1972 A numerical shallow fluid model including orography with a variable grid. *J. Atmos. Sci.* **29**, 270–284.
- VERRON, J. & LE PROVOST, C. 1985 A numerical study of quasi-geostrophic flow over isolated topography. *J. Fluid Mech.* **154**, 231–252
- WEI, M. & FREDERIKSEN, J. S. 2004 Error growth and dynamical vectors during southern hemisphere blocking. *Nonlinear Processes Geophys.* **11**, 99–118.